Dosimetric materials: what do we need to know?

Guerda Massillon-JL

massillon@fisica.unam.mx

Instituto de Física, UNAM, México

How can we know the absorbed dose?

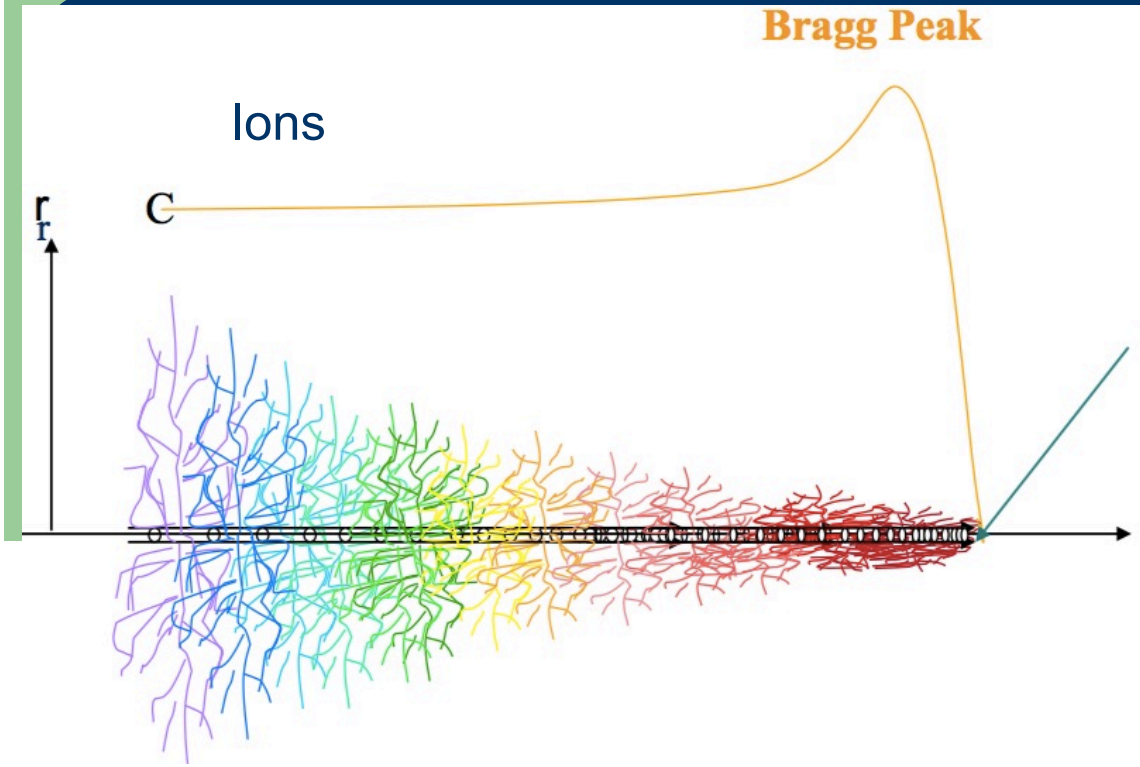

Massillon-JL, PhD Thesis UNAM 2006

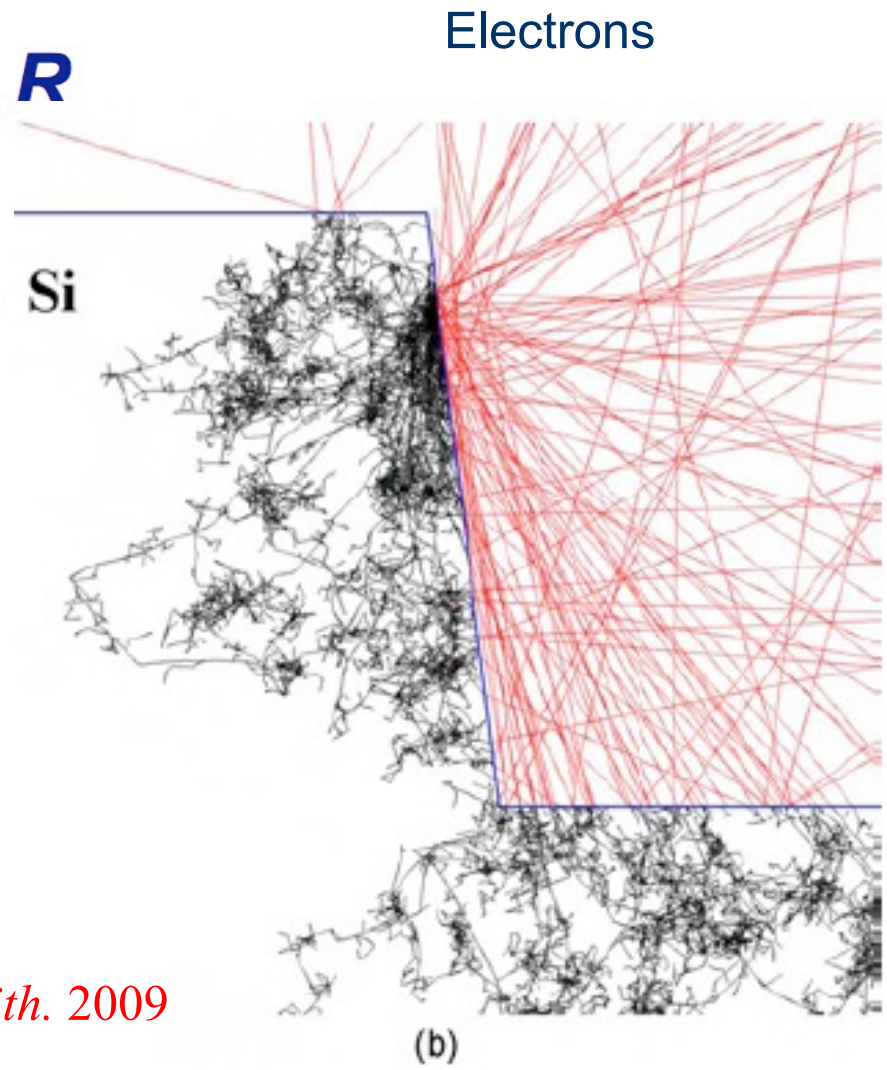

Generation of secondary electron (SE) cascades

Villarrubia and Ding, *J. Micro/Nanolith.* 2009

Millions of questions ?

Part I

How do these electrons interact with matter?

How many are produced during the interaction?

What is their range?

Irradiated mass?

Part II

Where are the electrons localized?

Is all the energy transformed into a response?

Part I: Cross sections

Electron beam–solid-state interaction model

Interaction between the charge and spin of an incident particle and those of atomic electrons

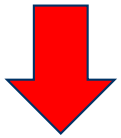

Relativistic differential cross section (DCS) for inelastic scattering from quantum theory has two components:

1. Longitudinal excitation: The Coulomb interaction exerts a force parallel to the momentum transfer, q.
2. Transverse excitation: Interaction through virtual photons that are perpendicular to q (negligible at T < 500 keV)

U Fano, *Ann. Rev. Nucl. Sci.* 13 1 (1963)

Part I: Cross-sections

DCS for the longitudinal excitation in terms of the momentum transfer, q

$$\frac{d^2\sigma_L}{d\omega dq} = \frac{2}{\pi N v^2}\,\mathbf{Im}\left[\frac{-1}{\epsilon(q,\omega)}\right]\frac{1}{q}, \qquad \lambda^{-1} = N\sigma$$

$$\frac{d^2\lambda^{-1}}{d\omega dq} = \frac{2}{\pi\, v^2}\,\mathrm{Im}\left[\frac{-1}{\epsilon(q,\omega)}\right]\frac{1}{q}$$

N: number density of scatterers

ω and q: energy and momentum transfer

v: incident electron's speed

$\epsilon(q,\omega)$: momentum and energy-dependent dielectric function

$\mathrm{Im}[-1/\epsilon(q,\omega)]$: energy loss function (ELF)

U Fano, *Ann. Rev. Nucl. Sci.* 13 1 (1963)

Part I: Cross-sections

The inelastic mean free path (IMFP), λ for an electron can be expressed as

$$\lambda^{-1} = \frac{(1 + T'/c^2)^2}{1 + T'/2c^2} \frac{\mathbf{1}}{\boldsymbol{\pi}\, T'} \int_{\omega_{\min}}^{T'-w_{\mathrm{VB}}} \int_{q^-}^{q^+} \mathbf{Im}\left[\frac{-1}{\epsilon(q,\omega)}\right] \frac{dq}{q} d\omega$$

$$q^{\pm} = \sqrt{T'(2 + T'/c^2)} \pm \sqrt{(T' - \omega)(2 + (T' - \omega)/c^2)}$$

w_{VB}: width of the valence band

$\omega_{\min}$: energy required to promote an electron from the top of the valence band to the bottom of the conduction band

MA Flores-Mancera *et al.* ASC Omega **5** (2020) 4139−4147

Part I: Stopping power

The stopping power can be calculated from the probability for an electron with relativistic kinetic energy, T, to loss energy per unit distance travelled as:

$$SP = \frac{\left(1+T'/c^2\right)^2}{1+T'/2c^2}\frac{1}{\pi\, T'}\int_{\omega_{\min}}^{T'-w_{\mathrm{VB}}}\int_{q_-}^{q_+}\mathbf{Im}\left[\frac{-1}{\epsilon(q,\omega)}\right]\frac{dq}{q}\omega \mathrm{d}\omega,$$

$$q_{\pm} = \sqrt{T'(2+T'/c^2)} \pm \sqrt{(T'-\omega)(2+(T'-\omega)/c^2)}$$

$T' = T - E_{\mathrm{g}}$,

E_{g}: the bandgap energy

c: the speed of light,

w_{VB}: the valence band width

$T' - w_{\mathrm{VB}}$: to assure that the incident electron preserves enough energy to stay in the conduction band

$\omega_{\min}$: the minimum energy required to promote an electron from the top of the valence band to the bottom of the conduction band

LR Castillo-Rico *et al.* Nucl. Instr. Methods Phys. B 502 (2021)189-197

Part I: Full Penn algorithm (NIST)

$$\mathbf{Im}\left[\frac{-1}{\epsilon(q,\omega)}\right] = -\int_0^\infty d\omega_p G(\omega_p)\,\mathbf{Im}\left[\frac{-1}{\epsilon_L(q,\omega;\omega_p)}\right],$$

$$G(\omega_p) = -\frac{2}{\pi\omega_p}\mathbf{Im}\left[\frac{-1}{\epsilon(\omega_p)}\right]$$

Due to some limitation on the Lindhard energy loss function, the ELF can be portrayed as a combination of the plasmon pole and the single-electron excitations such as:

$$\mathbf{Im}\left[\frac{-1}{\epsilon(q,\omega)}\right] = \mathbf{Im}\left[\frac{-1}{\epsilon(q,\omega)}\right]_{pl} + \mathbf{Im}\left[\frac{-1}{\epsilon(q,\omega)}\right]_{se}$$

Shinotsuka et al., *Surf. Interface Anal.* 47 871 (2015)

Part I: Full Penn algorithm (NIST)

$$\mathbf{Im}\left[\frac{-1}{\epsilon(q,\omega)}\right]_{pl} = G(\omega_0)\frac{\pi}{\left[\partial\epsilon_L(q,\omega;\omega_p)/\partial\omega_p\right]_{\omega_p=\omega_0}}\theta(q^-(\omega;\omega_0)-q),$$

$$q^{\pm}(\omega;\omega_0) = \pm\left[\omega_p\left(\frac{3\pi}{4}\right)^{1/2}\right]^{1/3} + \left[\omega_p{}^{\frac{2}{3}}\left(\frac{3\pi}{4}\right)^{\frac{1}{3}} + 2\omega\right]^{\frac{1}{2}}$$

$$\mathbf{Im}\left[\frac{-1}{\epsilon(q,\omega)}\right]_{se} = \int_0^{\infty} d\omega_p G(\omega_p)\,\mathbf{Im}\left[\frac{-1}{\epsilon_L(q,\omega;\omega_p)}\right]\theta\left(q^+(\omega;\omega_p)-q\right)\theta\left(q-q^-(\omega;\omega_p)\right)$$

Shinotsuka et al., *Surf. Interface Anal.* 47 871 (2015)

JMONSEL vs Experiment

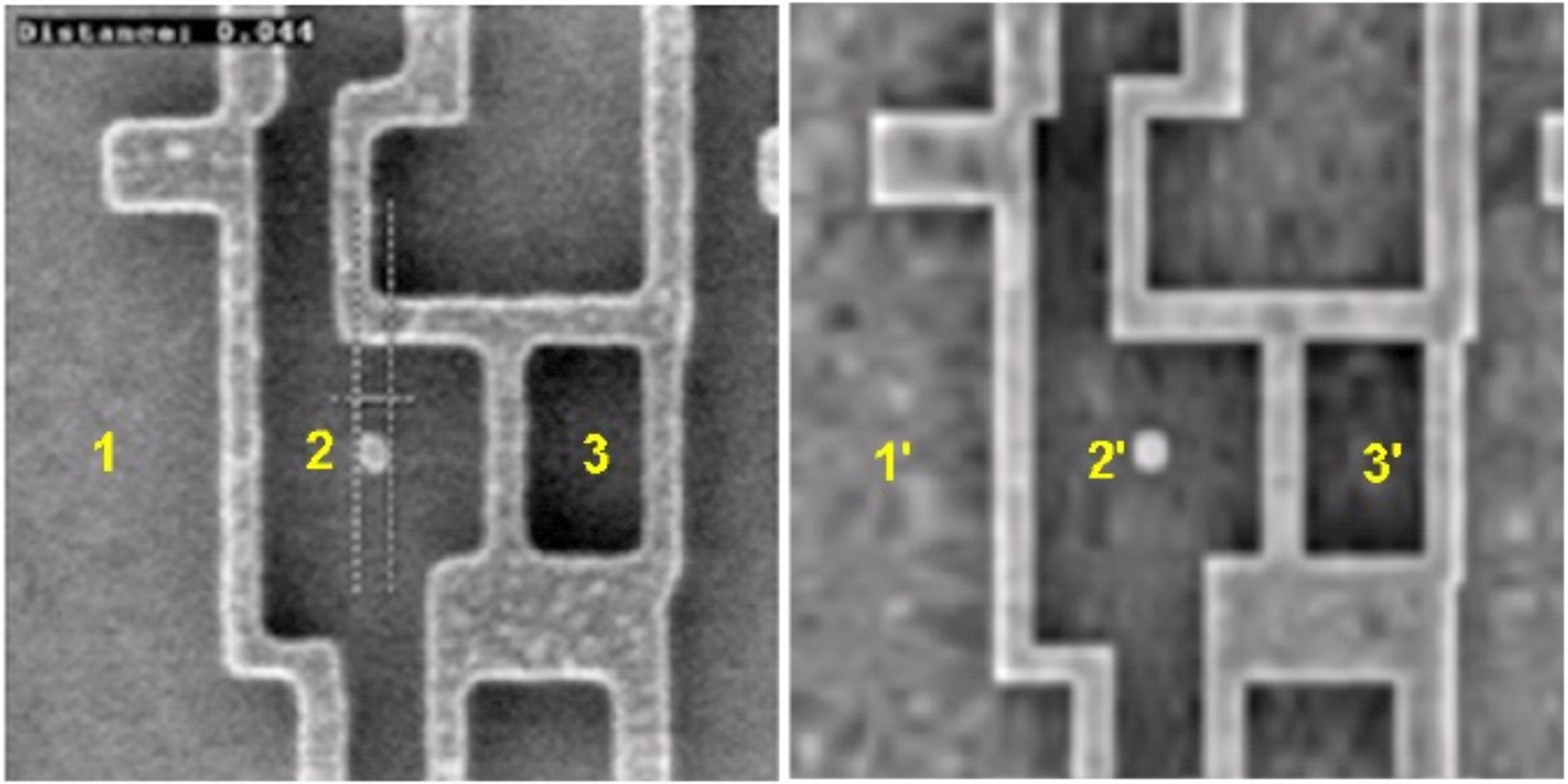

Figure 7. Comparison of measured (left, SEM image, courtesy SEMATECH) and simulated (right) images of an intentional defect array structure. Neighborhoods 1, 2, and 3 (1', 2', and 3' in the simulation) are progressively more confined and also progressively darker. 1 μm fields of view (Figure reproduced from reference 10).

Scanning electron microscopy (SEM) Vladár *et al.* Proc. of SPIE **8324** 832402-1 (2012)

Consistency in the optical data

$$P_{\text{eff}} = \frac{2}{\pi}\int_0^{\omega_{max}} \frac{\mathbf{Im}\left(-\frac{1}{\epsilon(\omega)}\right)}{\omega} d(\omega)\Bigg) + n(0)^{-2}$$

$$Z_{\text{eff}} = -\frac{2m\epsilon_0}{\pi N e^2}\int_0^{\omega_{max}} \omega \mathbf{Im}\left[\frac{1}{\epsilon(\omega)}\right] d(\omega),$$

Table 1. *KK-sum* and *f-sum* errors.

Compound	n(0)	Z	Z_{eff}	f-sum error (%)	P_{eff}	KK-sum error (%)
H_2O	8.97	10	10.021	0.21	1.027	2.7
LiF	3	12	13.16	9.69	1.132	13.2
CaF_2	2.6	38	38.91	2.4	1.058	5.8
Al_2O_3	3.13	50	51.58	3.16	1.038	3.8

MA Flores-Mancera *et al.* ASC Omega **5** (2020) 4139−4147

Energy-loss function

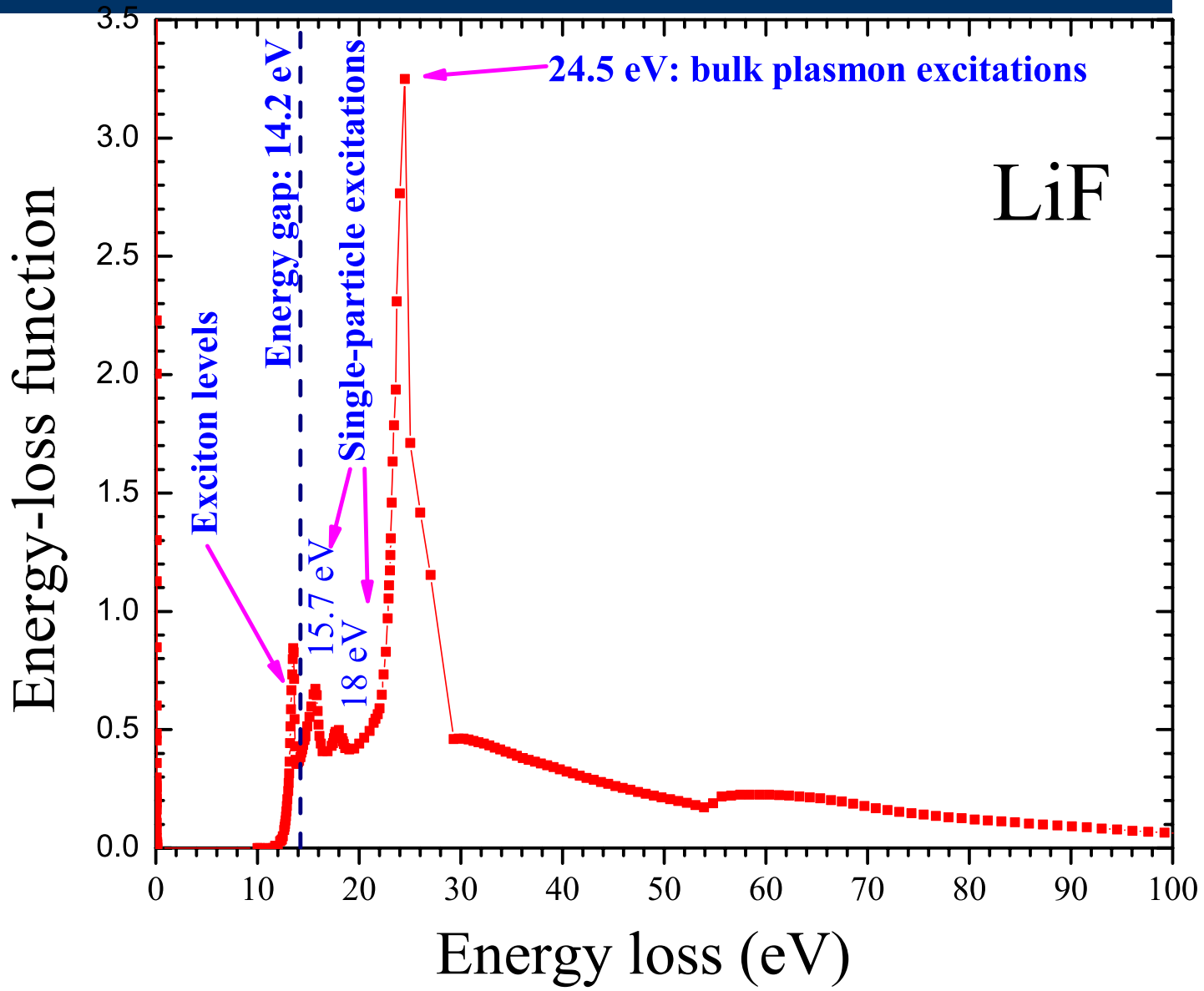

MA Flores-Mancera *et al.* ASC Omega **5** (2020) 4139−4147

ELF vs momentum vs energy loss

SPA

FPA

$q \neq 0$

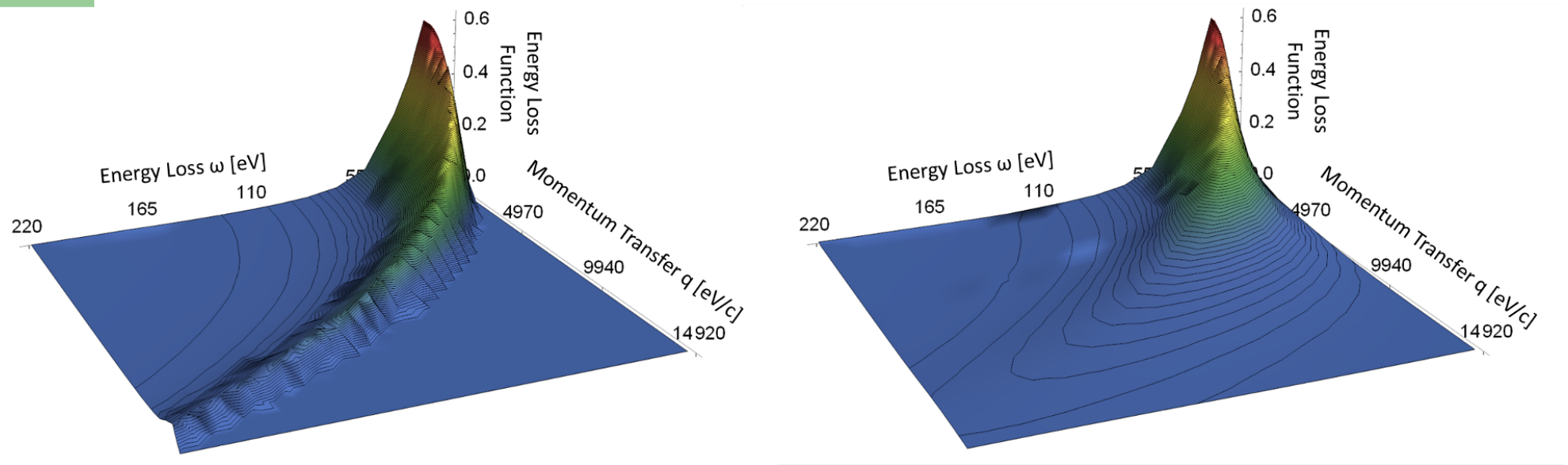

Perspective view of ELF as a function of momentum transfer and energy loss calculated by the FPA for liquid water

LR Castillo-Rico *et al.* Nucl. Instr. Methods Phys. B 502 (2021)189-197

Electron mean free path

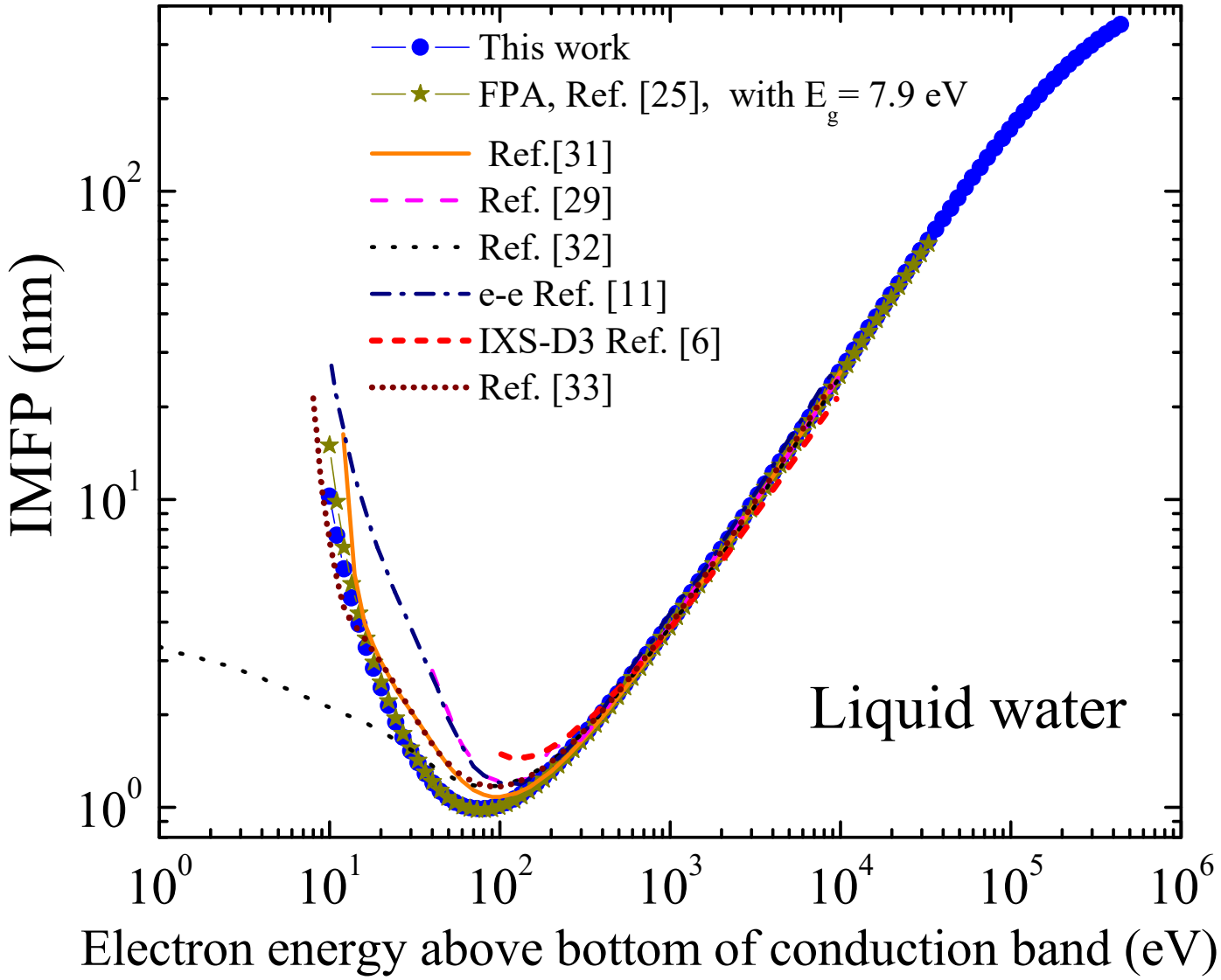

MA Flores-Mancera *et al.* ASC Omega **5** (2020) 4139−4147

Electron mean free path

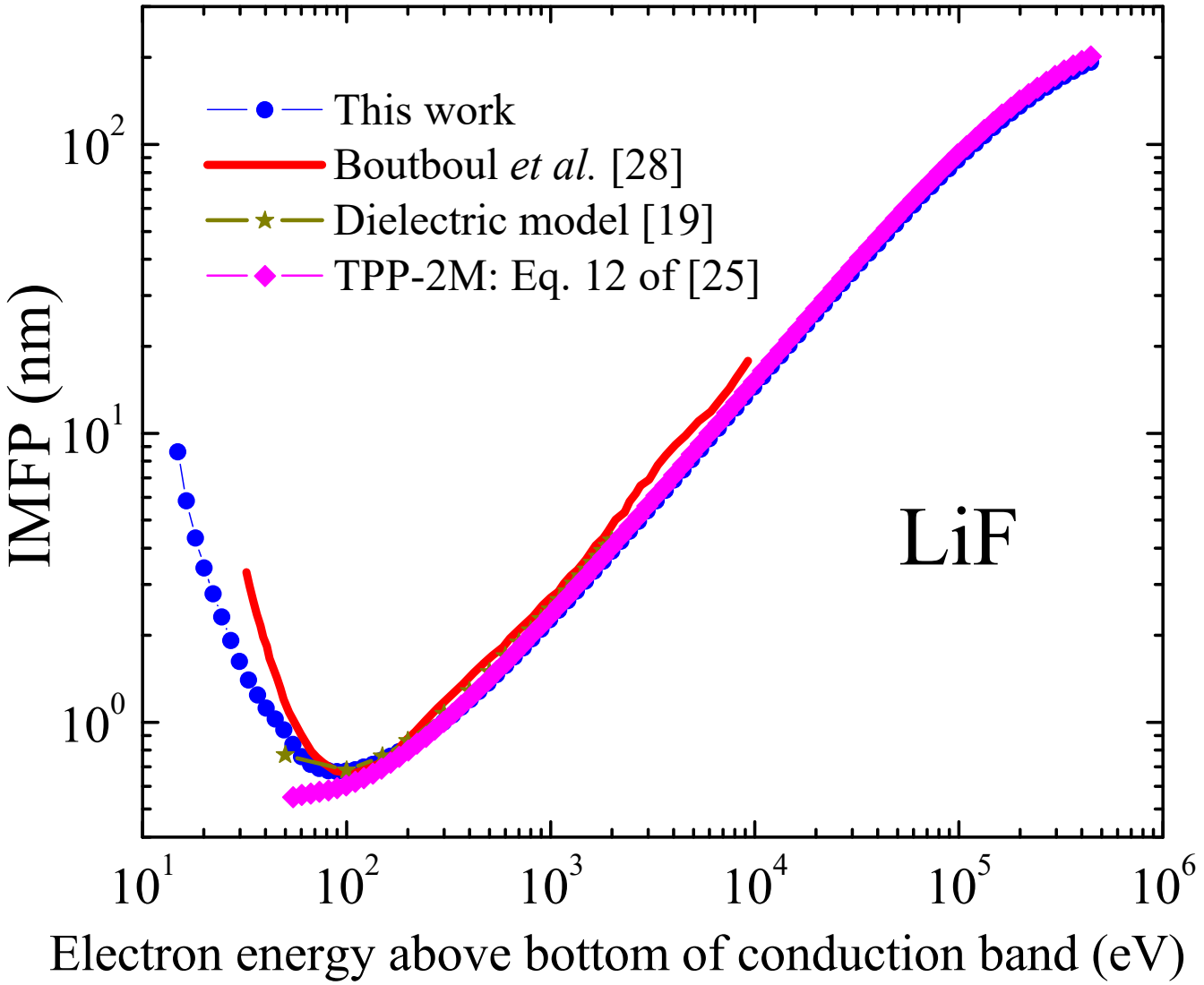

MA Flores-Mancera *et al.* ASC Omega **5** (2020) 4139−4147

Electron mean free path

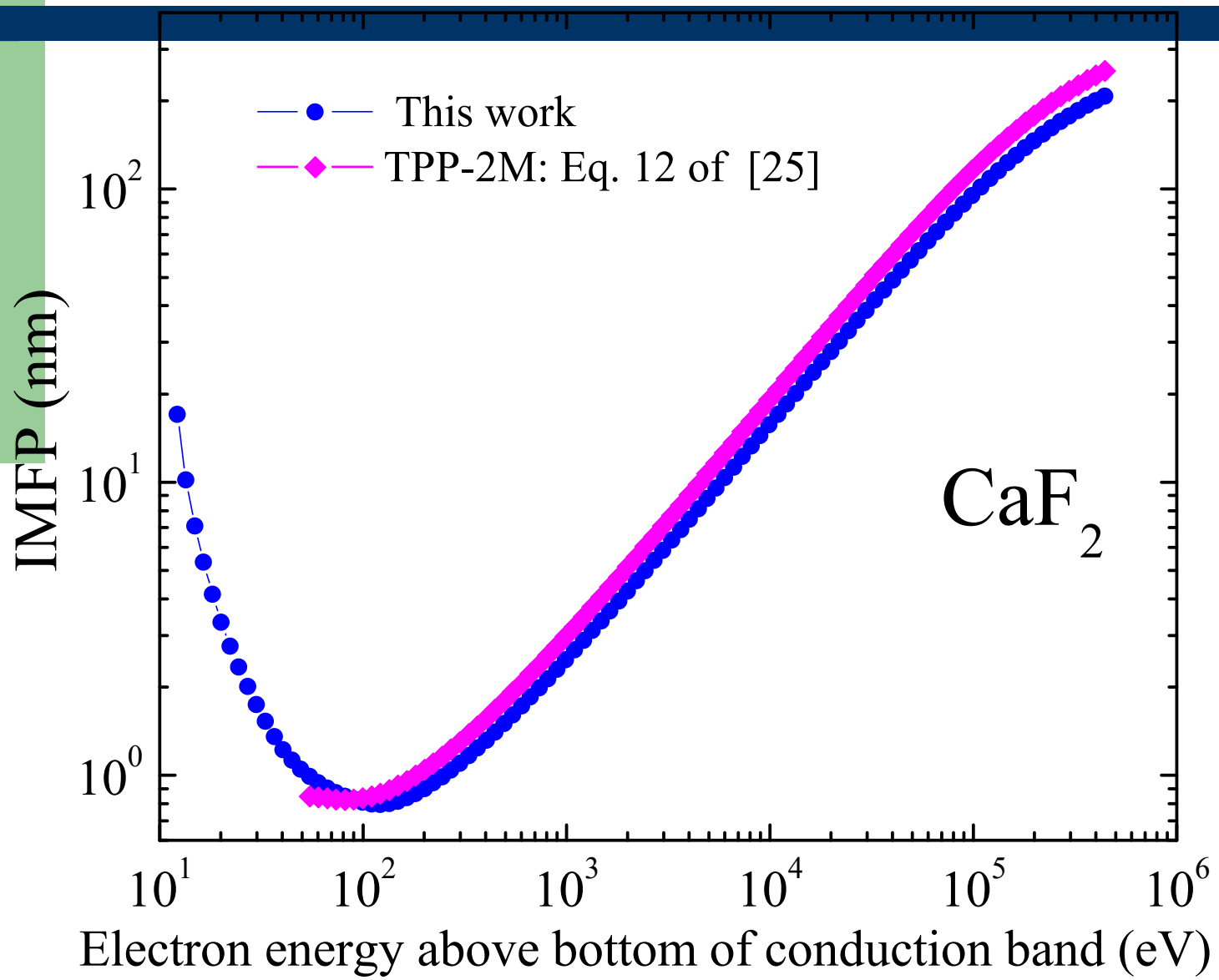

MA Flores-Mancera *et al.* ASC Omega **5** (2020) 4139−4147

Electron mean free path

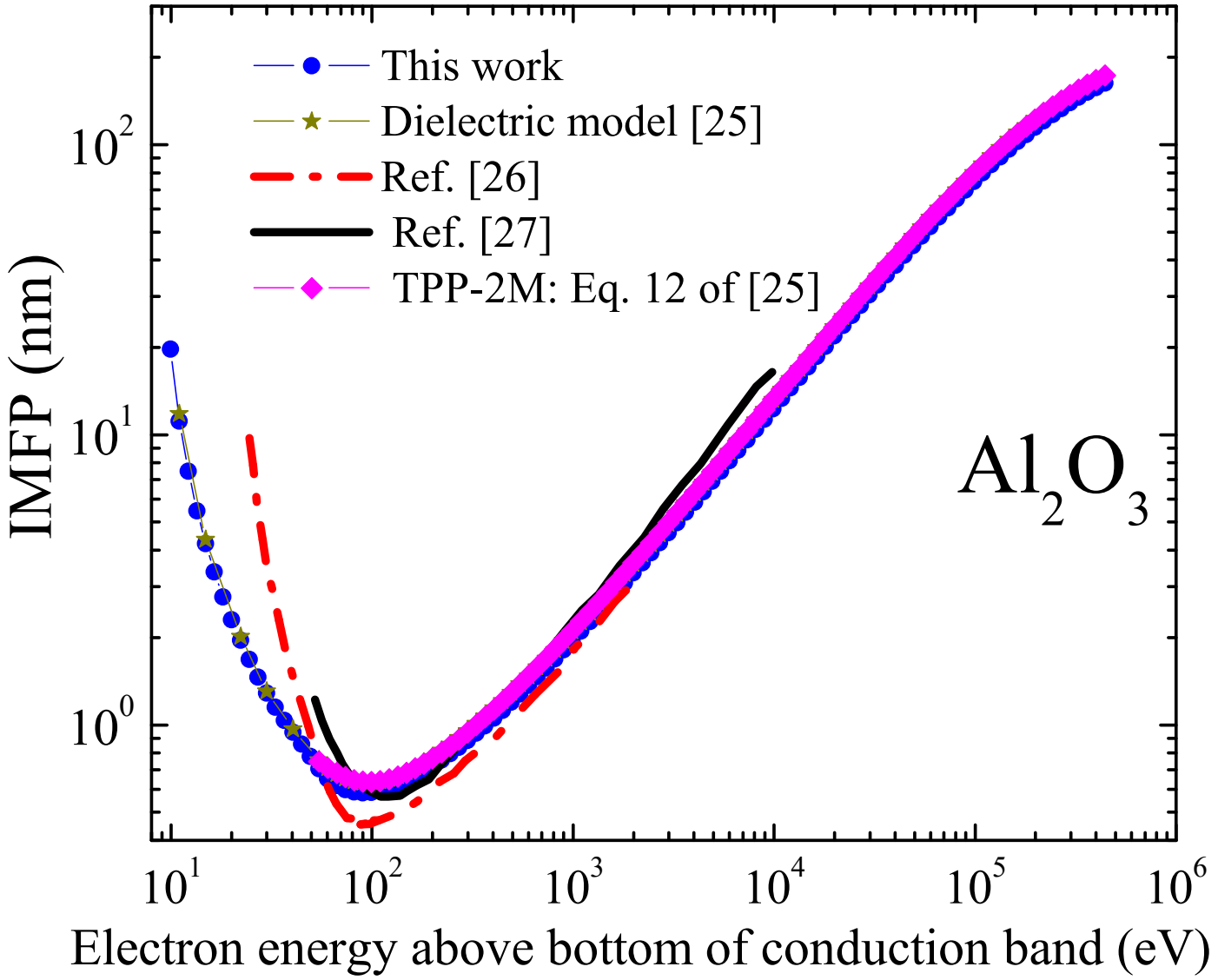

MA Flores-Mancera *et al.* ASC Omega **5** (2020) 4139−4147

Electron Stopping power using linear response: The dielectric model

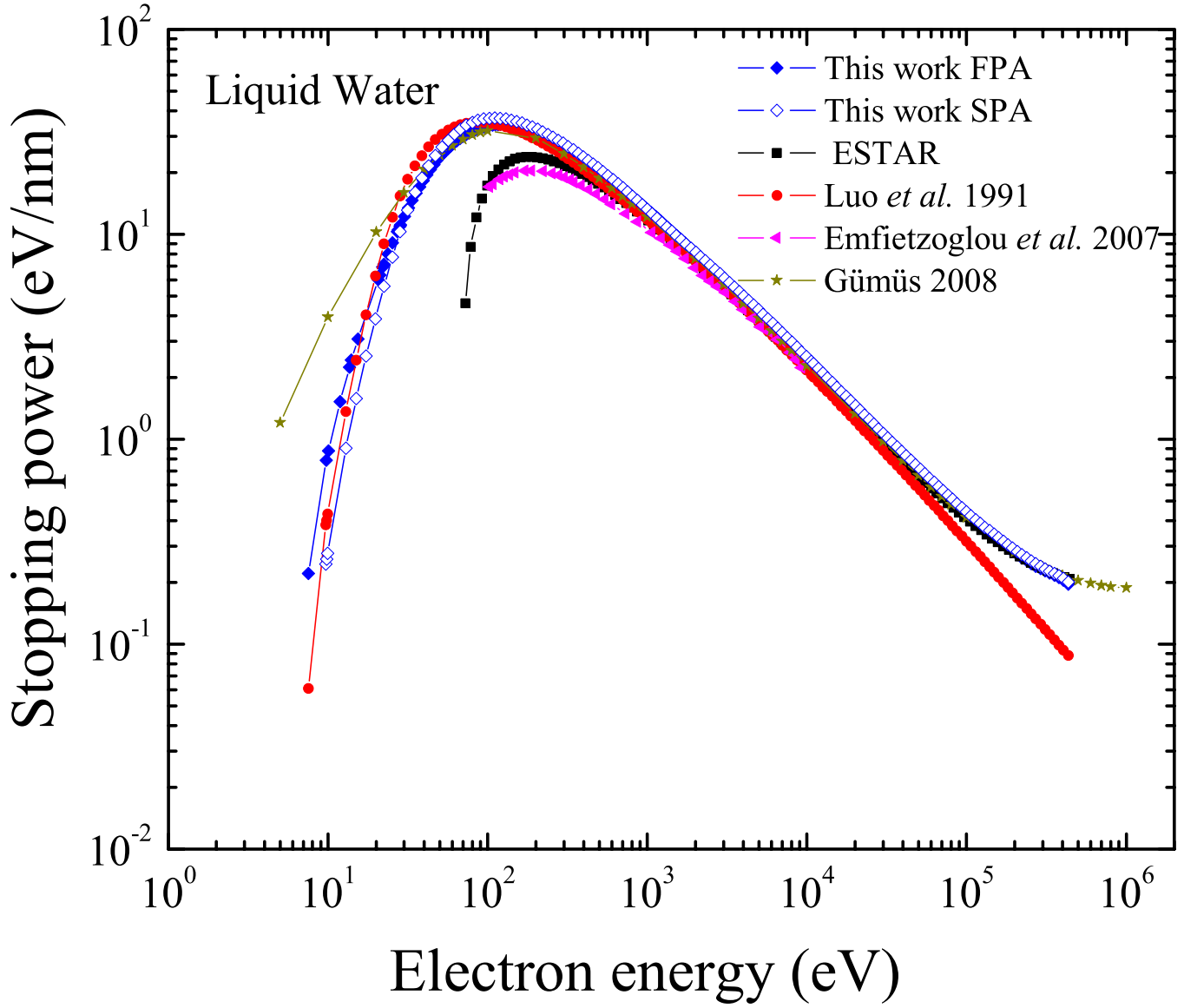

LR Castillo-Rico *et al.* Nucl. Instr. Methods Phys. B 502 (2021)189-197

Electron Stopping power using linear response: The dielectric model

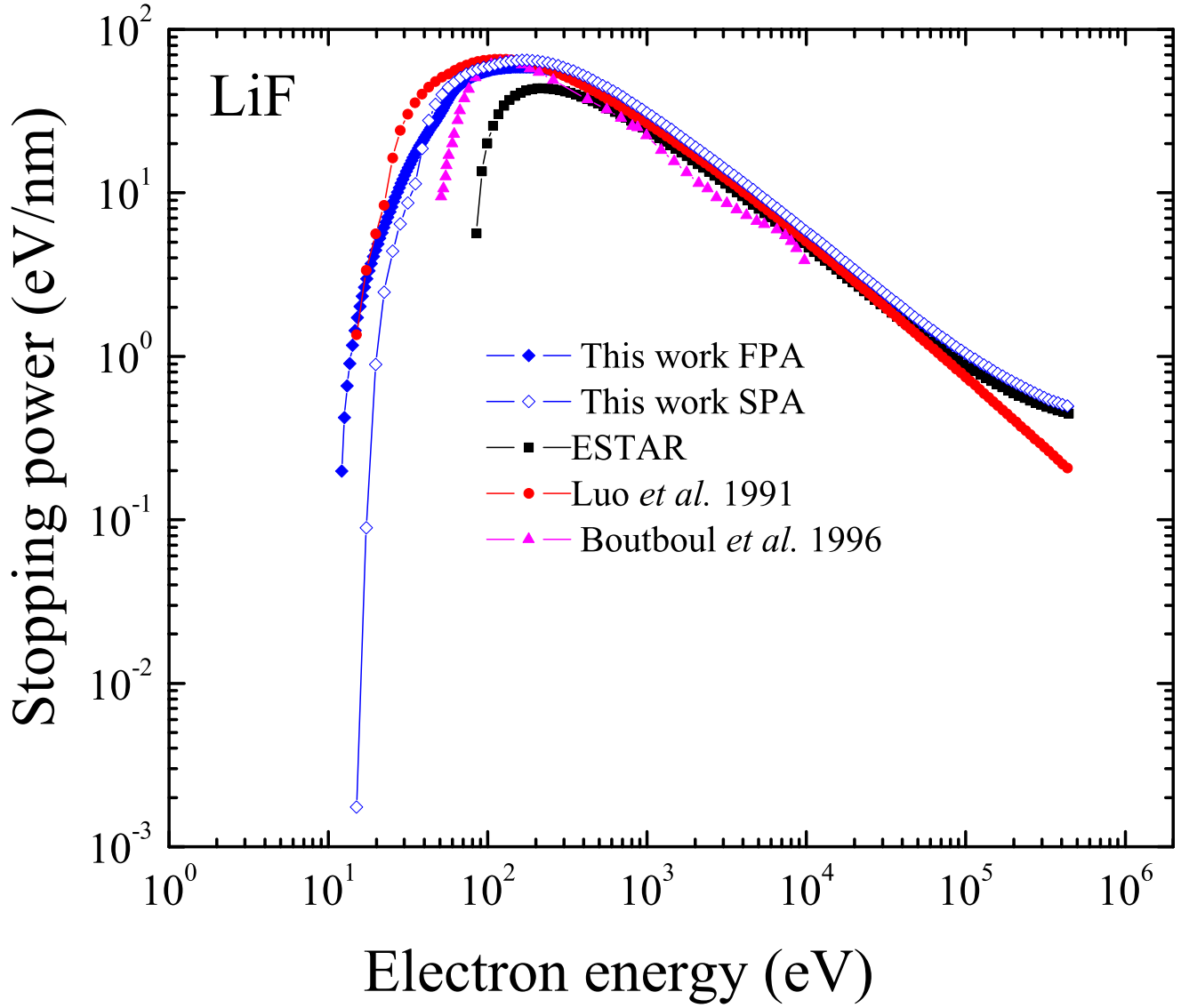

LR Castillo-Rico *et al.* Nucl. Instr. Methods Phys. B 502 (2021)189-197

Part II: LiF:Mg,Ti?

During the last few years, density functional theory (DFT) has been considered as a suitable tool to study radiation effects and electronic structures of:

Ti, Mg-doped LiF

Massillon-JL et *al. J. Phys.:Condens. Matter* **31** (2019) 025502
Massillon-JL et *al. Radiat. Meas.* **174** (2024) 107114

Modak and Modak, Computational Materials Science **202** (2022) 110977

Simplified illustrative structures for the initial configurations

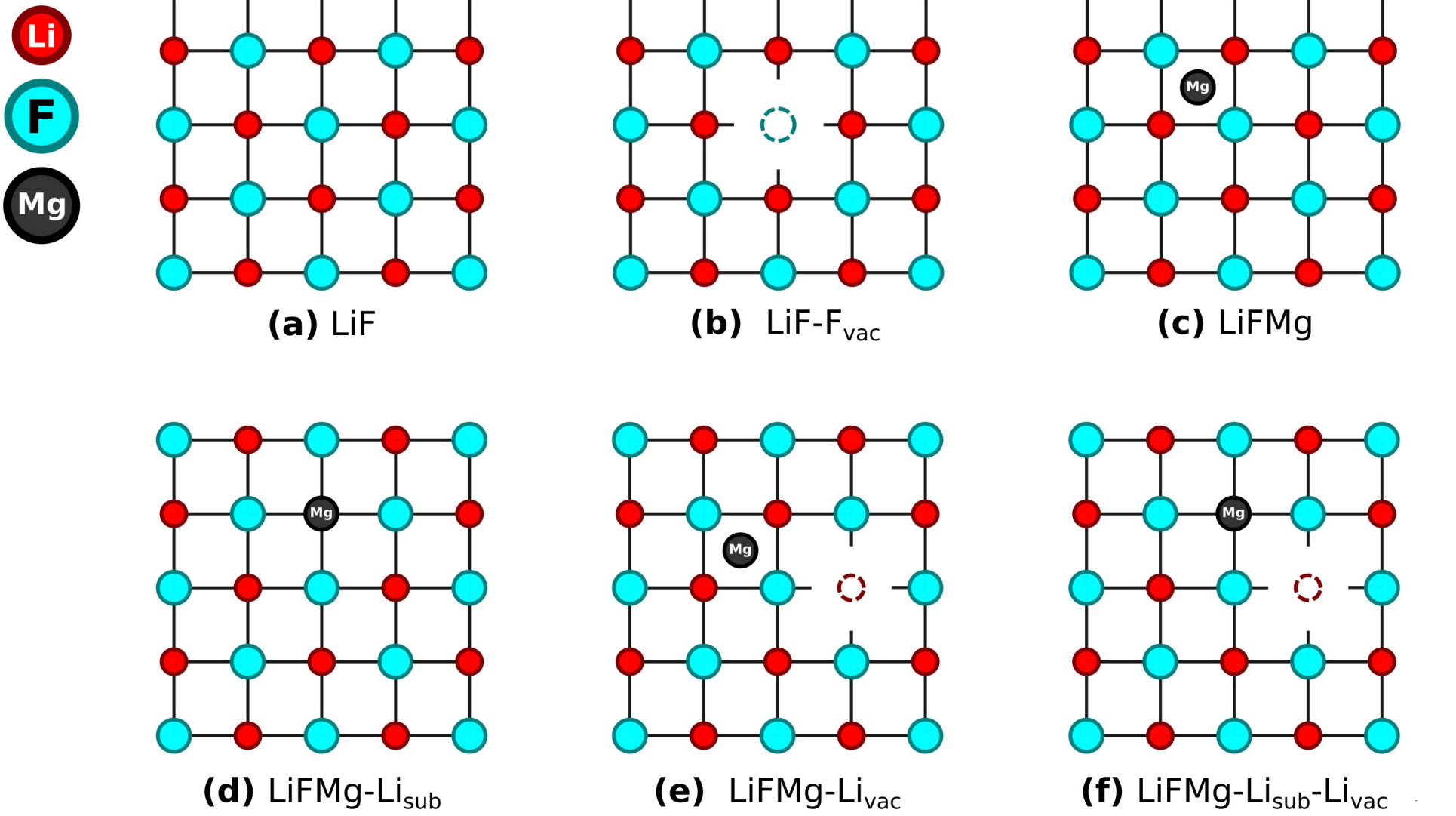

Massillon-JL et *al. J. Phys.:Condens. Matter* **31** (2019) 025502

Molecular dynamic simulation of LiF:Mg

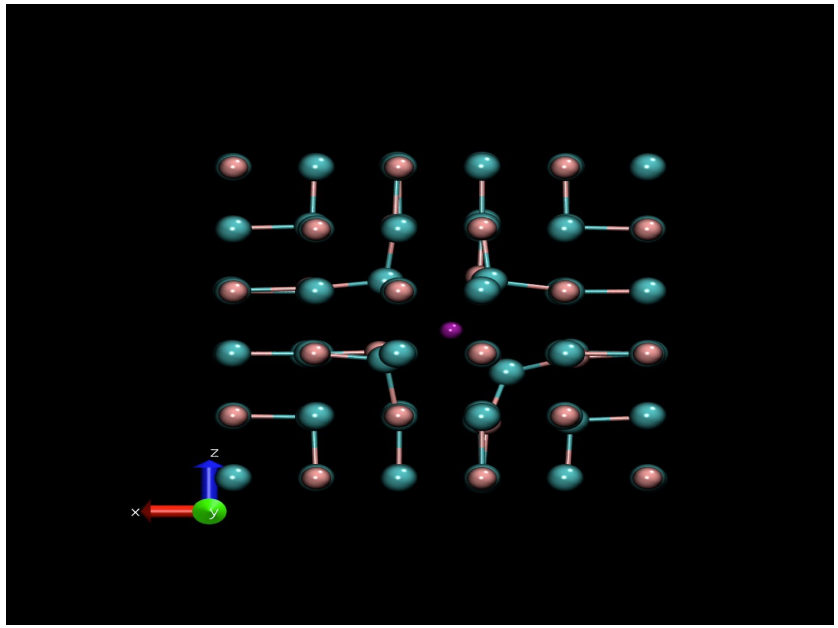

Massillon-JL et *al. J. Phys.:Condens. Matter* **31** (2019) 025502

Fluorine vacancy in LiF

Spin density isosurface of the LiF:F vacancy

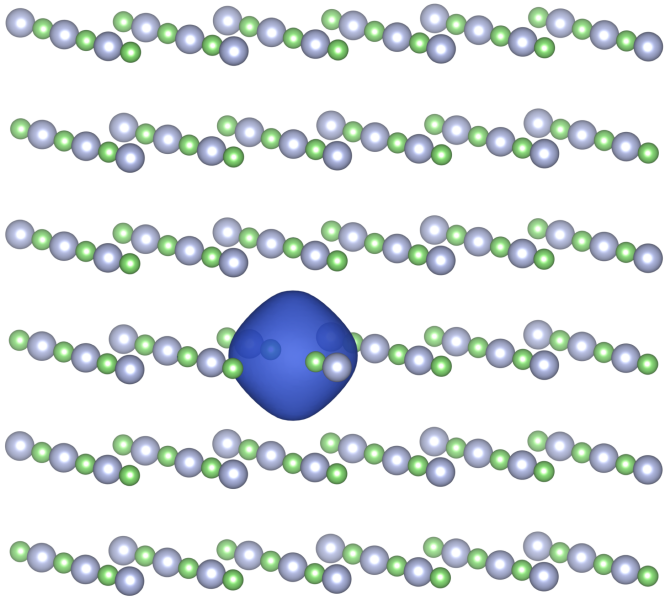

Two-dimensional contour plot of the F vacancy spin density

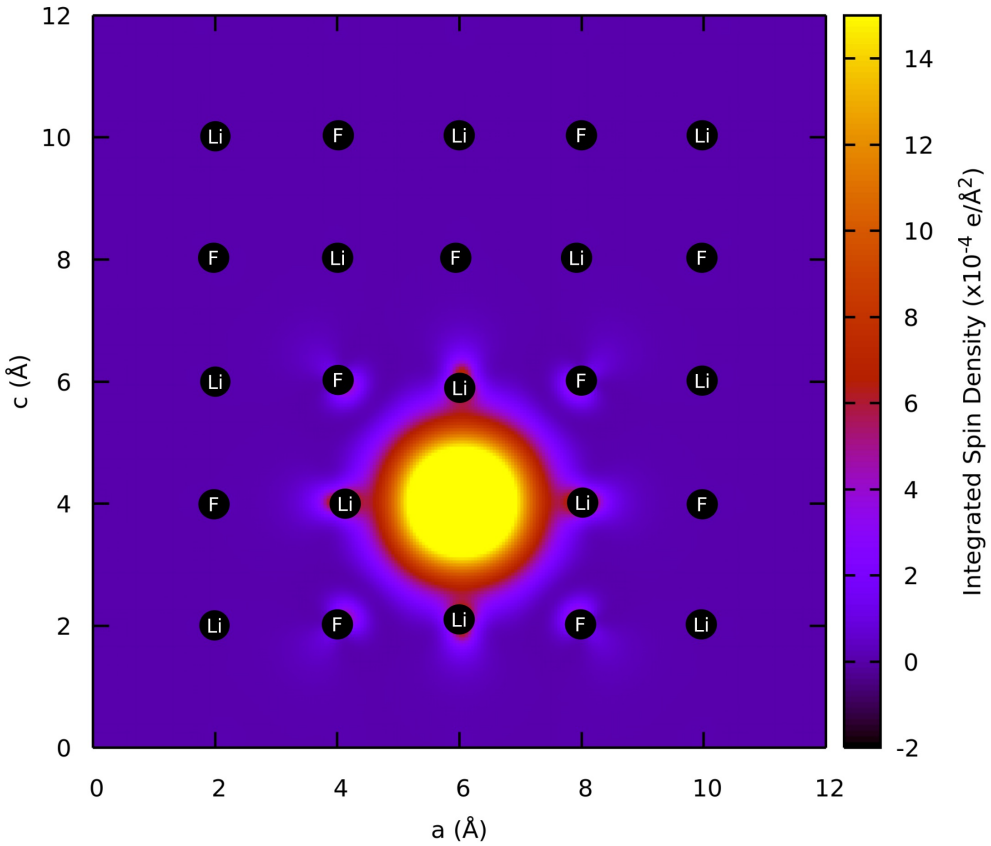

Massillon-JL et *al. J. Phys.:Condens. Matter* **31** (2019) 025502

Mg dopant in LiF

Spin density isosurface of the LiF:Mg with excess electron

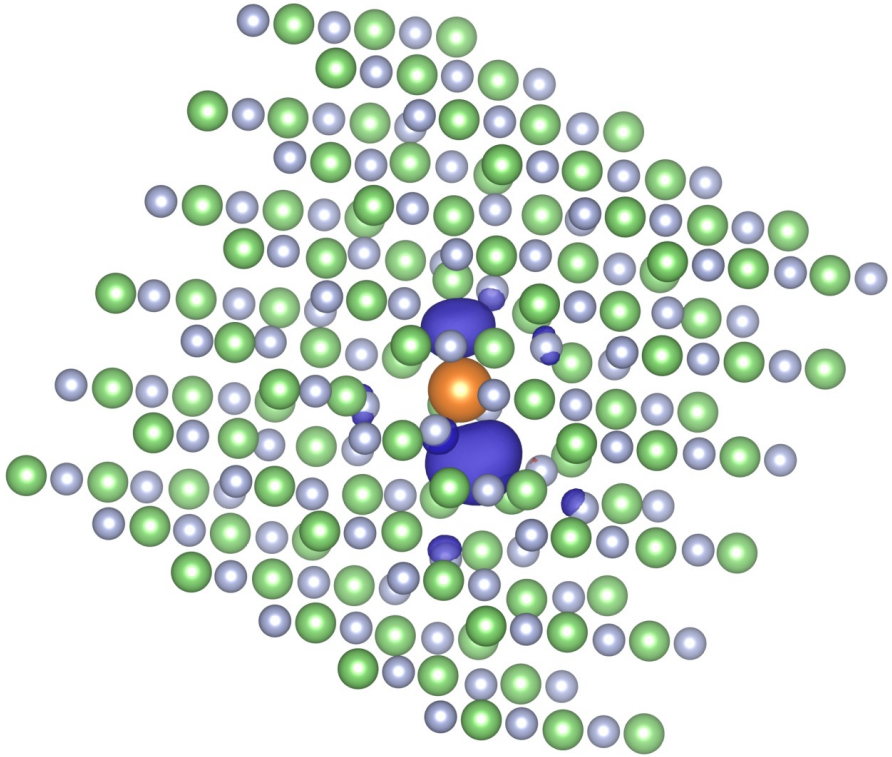

Two-dimensional contour plot of the LiF:Mg+e$^-$ spin density

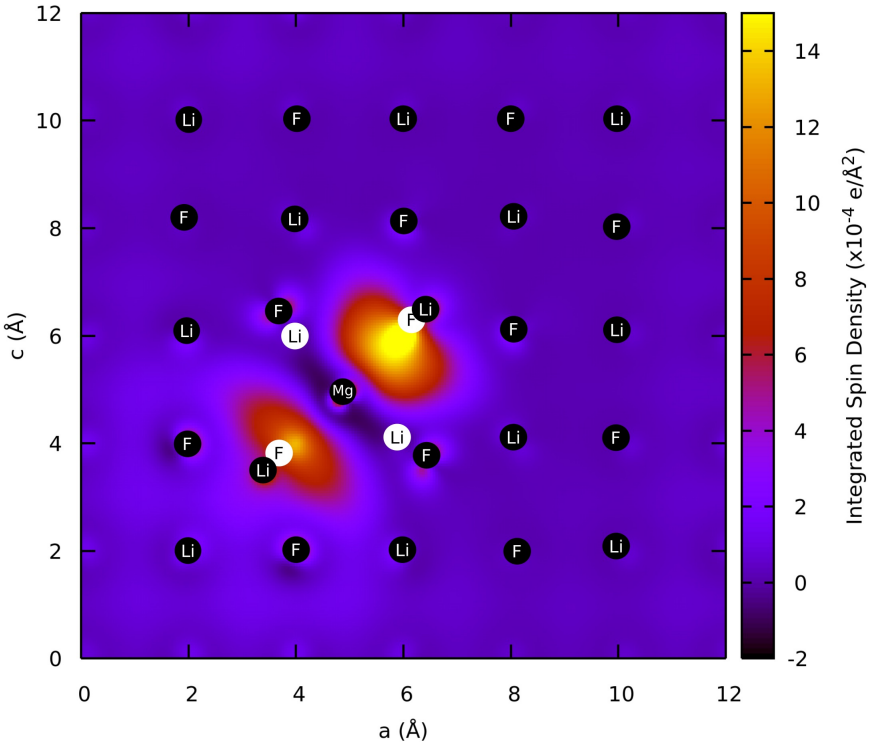

Massillon-JL et *al. J. Phys.:Condens. Matter* **31** (2019) 025502

Density of states for LiF:Mg

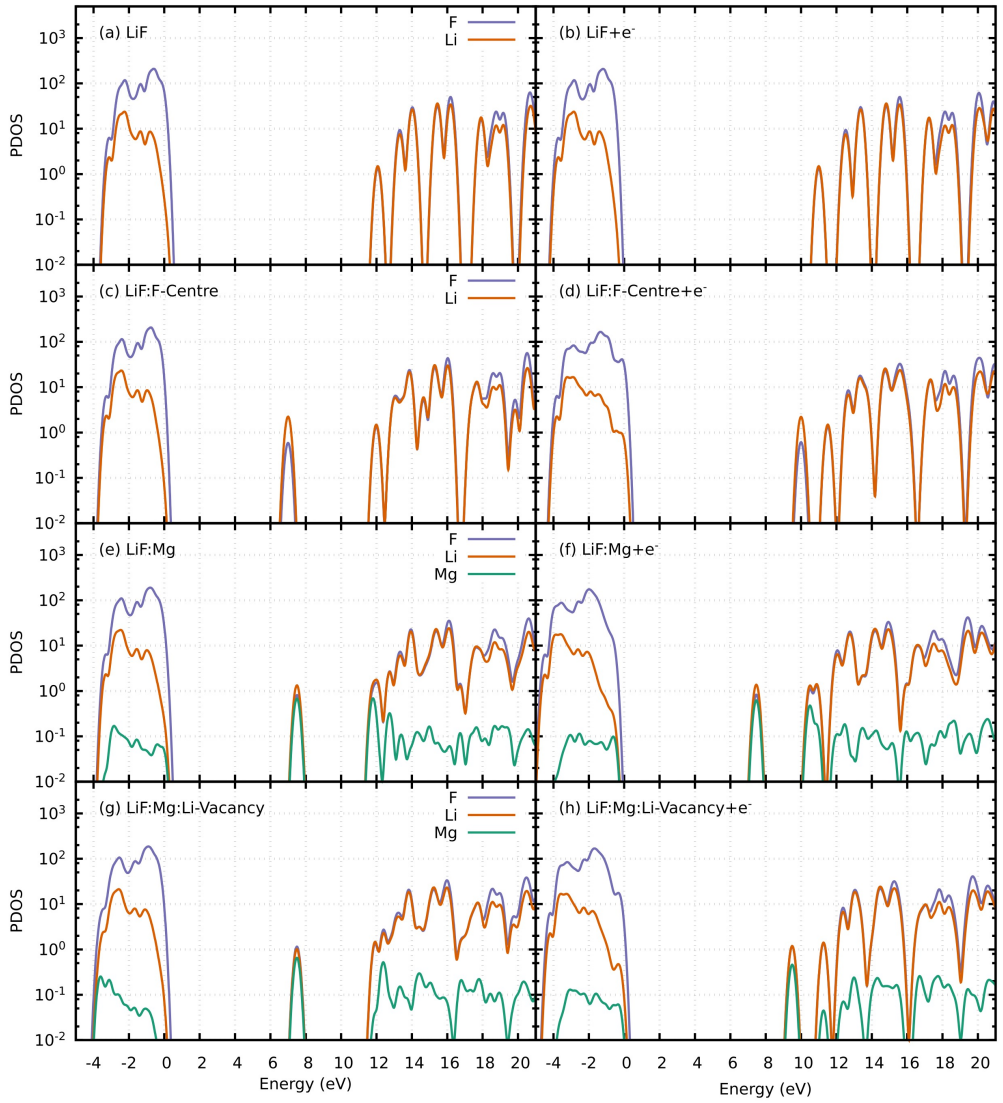

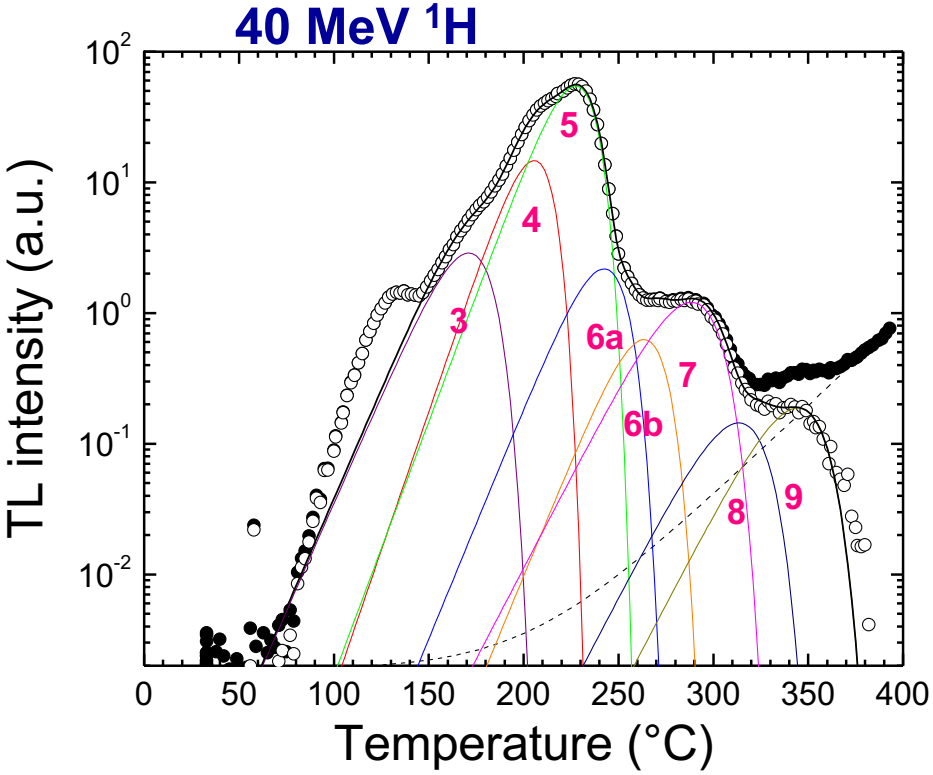

G Massillon-JL, PhD Thesis UNAM 2006

Massillon-JL et *al. J. Phys.:Condens. Matter* **31** (2019) 025502

Energy level of the defects in LiF:Mg

Table 1. Kohn–Sham energy levels of the defects, $E_{CBM} - E_{DS}$, in eV.

Defect-state	PBE	PBE0	Experiment
LiF-gap	9.06	12.075	14.2 + 2 [44]
F vacancy 1	3.420	5.064	5.061 [11]
F vacancy 2	1.629	1.866	—
LiF:Mg	2.270	4.534	4.428 [10–15]
$(LiF:Mg + e^-)^1$	2.268	4.865	—
$(LiF:Mg + e^-)^2$	—	4.224	4.000 [10–15]
$(LiF:Mg + e^-)^3$	—	2.688	
$(LiF:Mg–Li_{vac})^1$	2.557	4.487	
$(LiF:Mg–Li_{vac})^2$	1.461	1.584	
$LiF:Mg–Li_{vac} + e^-$	2.514	4.544	
$(LiF:Mg–Li_{sub})^1$	1.092	2.889	
$(LiF:Mg–Li_{sub})^2$	0.728	0.919	
$LiF:Mg–Li_{sub} + e^-$	1.785	3.486	3.263 [10–15]
$LiF:Mg–Li_{sub}–Li_{vac}$	—	—	
$(LiF:Mg–Li_{sub}–Li_{vac} + e^-)^1$	1.095	2.898	
$(LiF:Mg–Li_{sub}–Li_{vac} + e^-)^2$	0.730	0.922	

Massillon-JL et *al. J. Phys.:Condens. Matter* **31** (2019) 025502

Illustrative structure for the initial configuration of LiF:Ti

Atom symbols

- Grey: F
- Green: Li
- Cyan: Ti

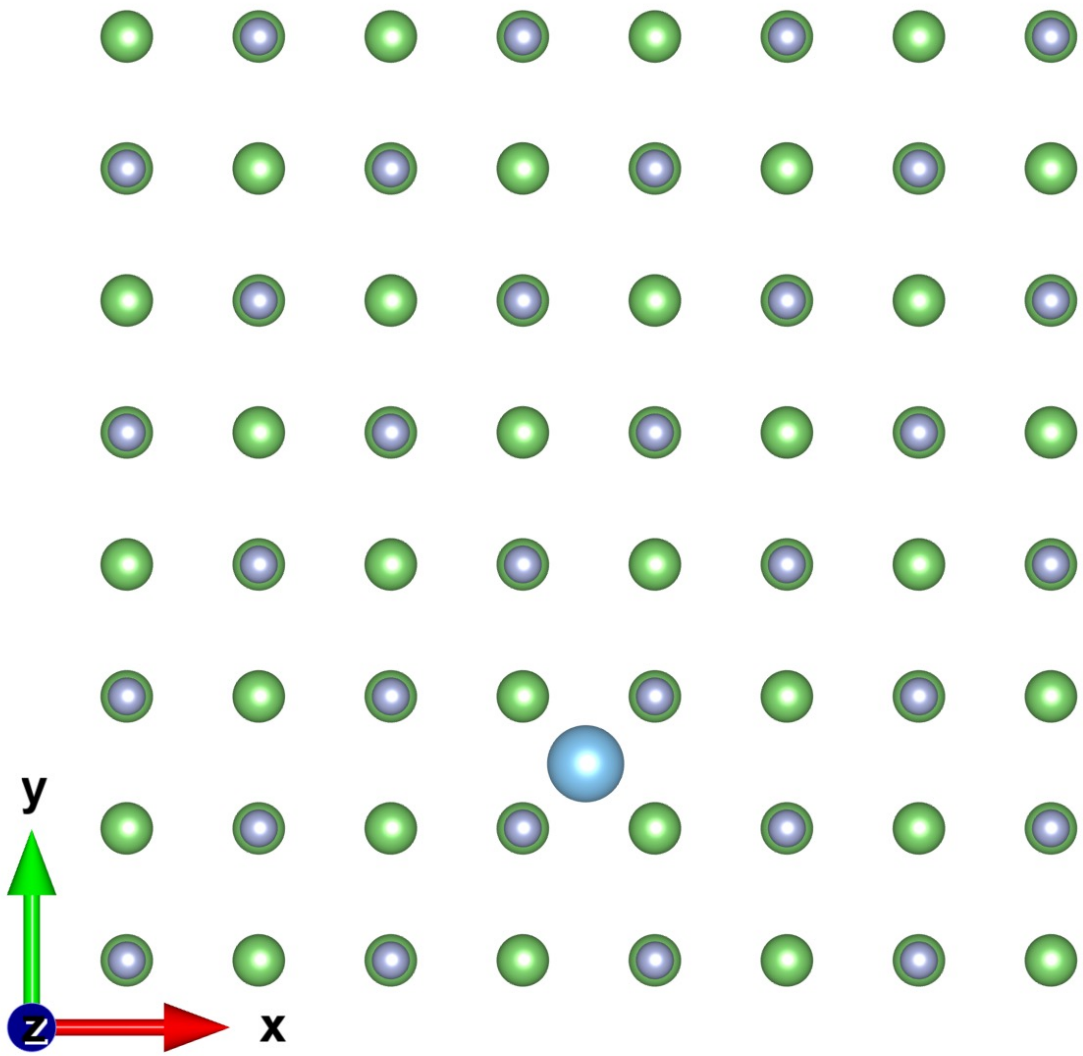

Massillon-JL et *al. Radiat. Meas.* **174** (2024) 107114

Geometry configuration of LiF:Ti after relaxation

Atom symbols

- Grey: F
- Green: Li
- Cyan: Ti

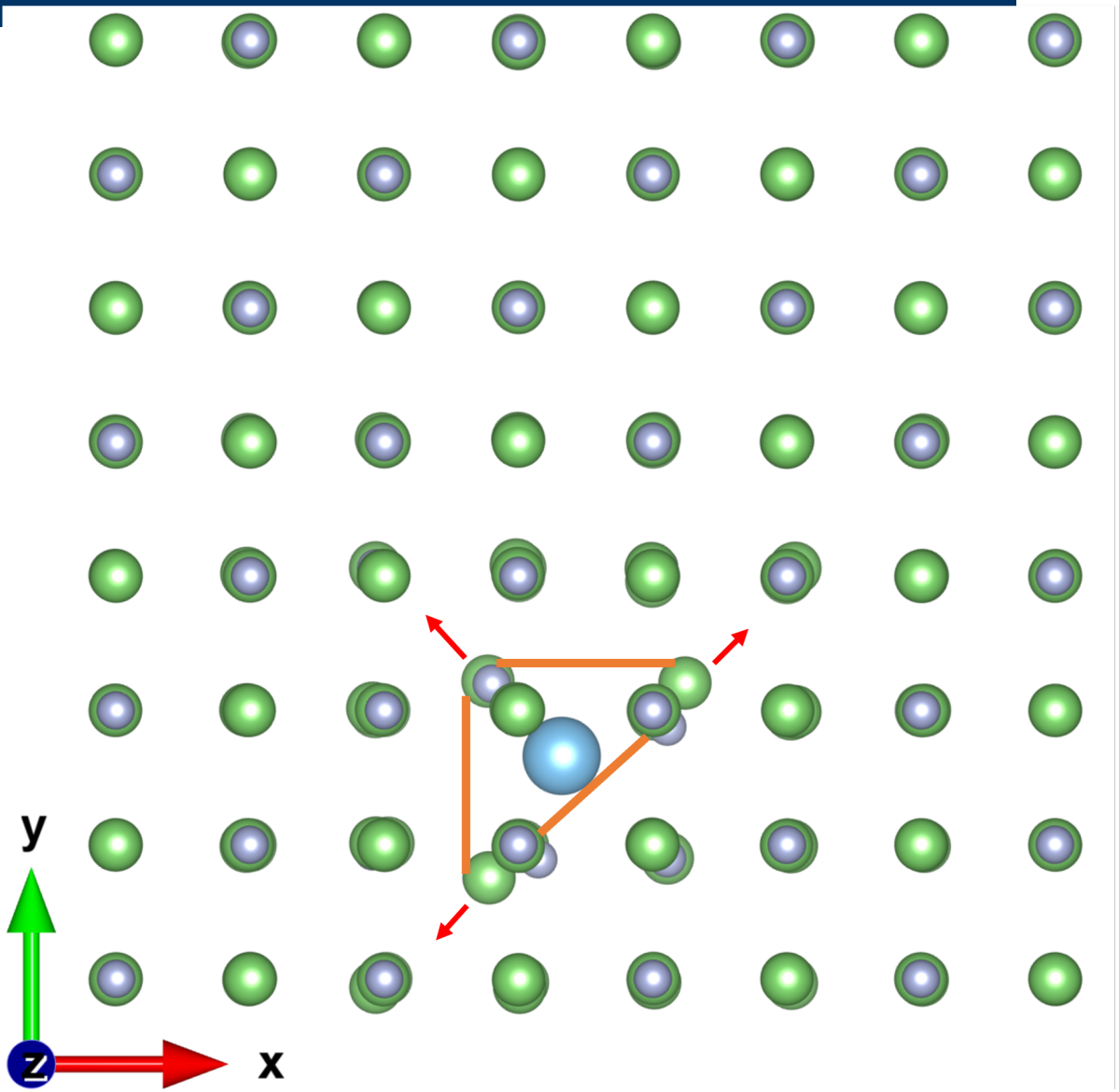

Massillon-JL et *al. Radiat. Meas.* **174** (2024) 107114

LiF:Ti with an excess electron after relaxation

Atom symbols

- Grey: F
- Green: Li
- Cyan: Ti

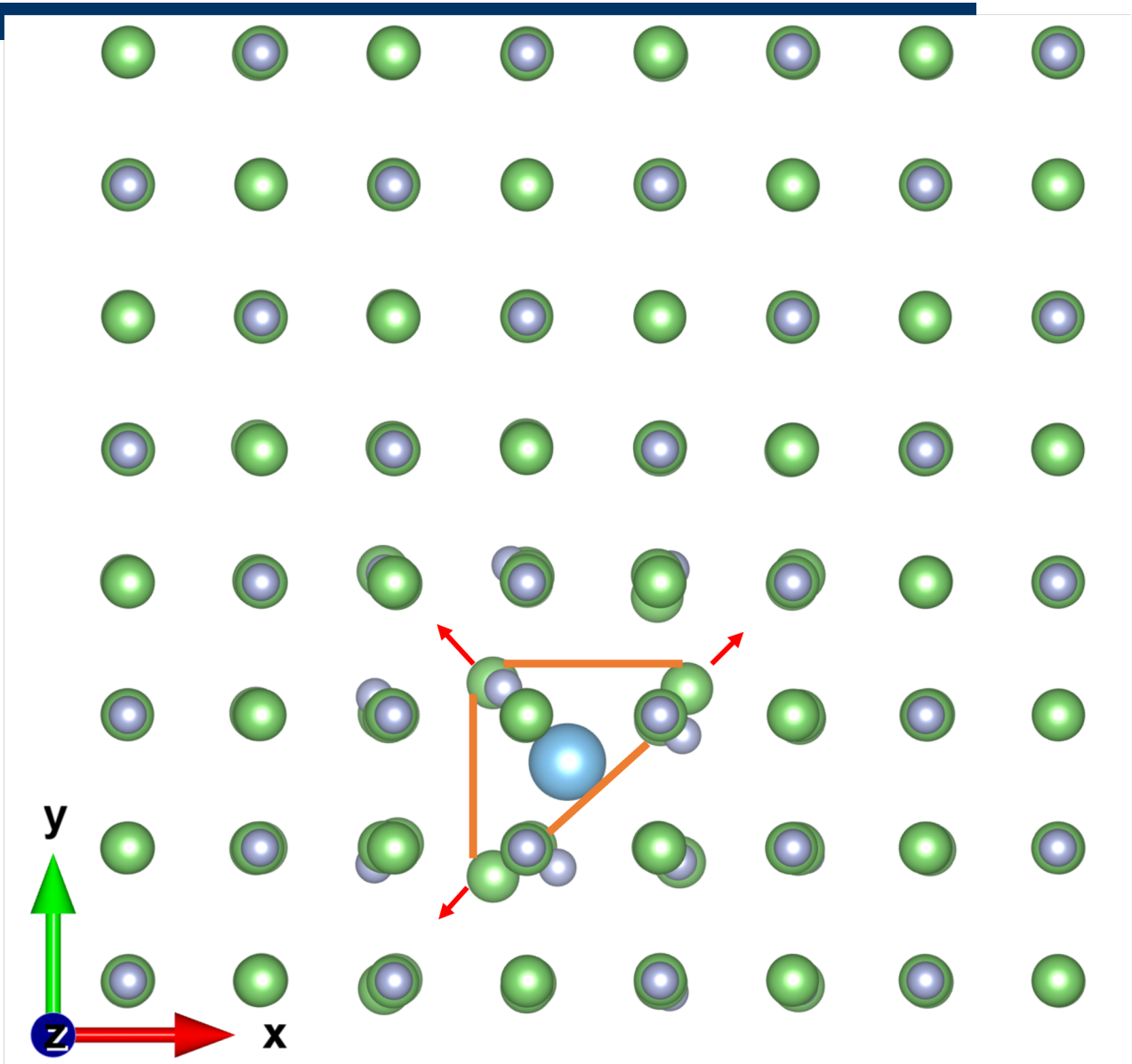

Massillon-JL et *al. Radiat. Meas.* **174** (2024) 107114

LiF:Ti with a hole after relaxation

Atom symbols

- Grey: F
- Green: Li
- Cyan: Ti

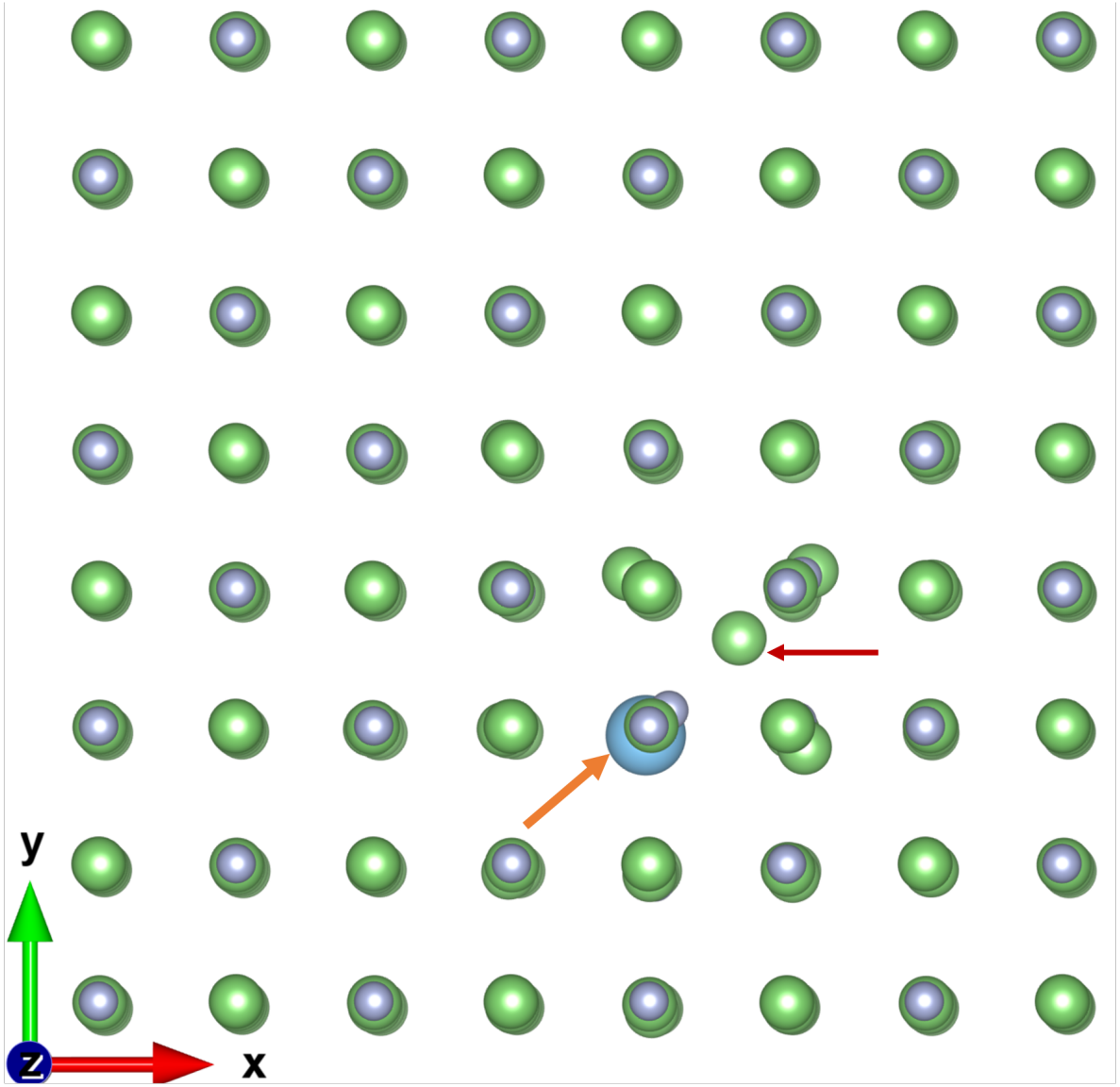

Massillon-JL et *al. Radiat. Meas.* **174** (2024) 107114

Density of states for LiF:Ti

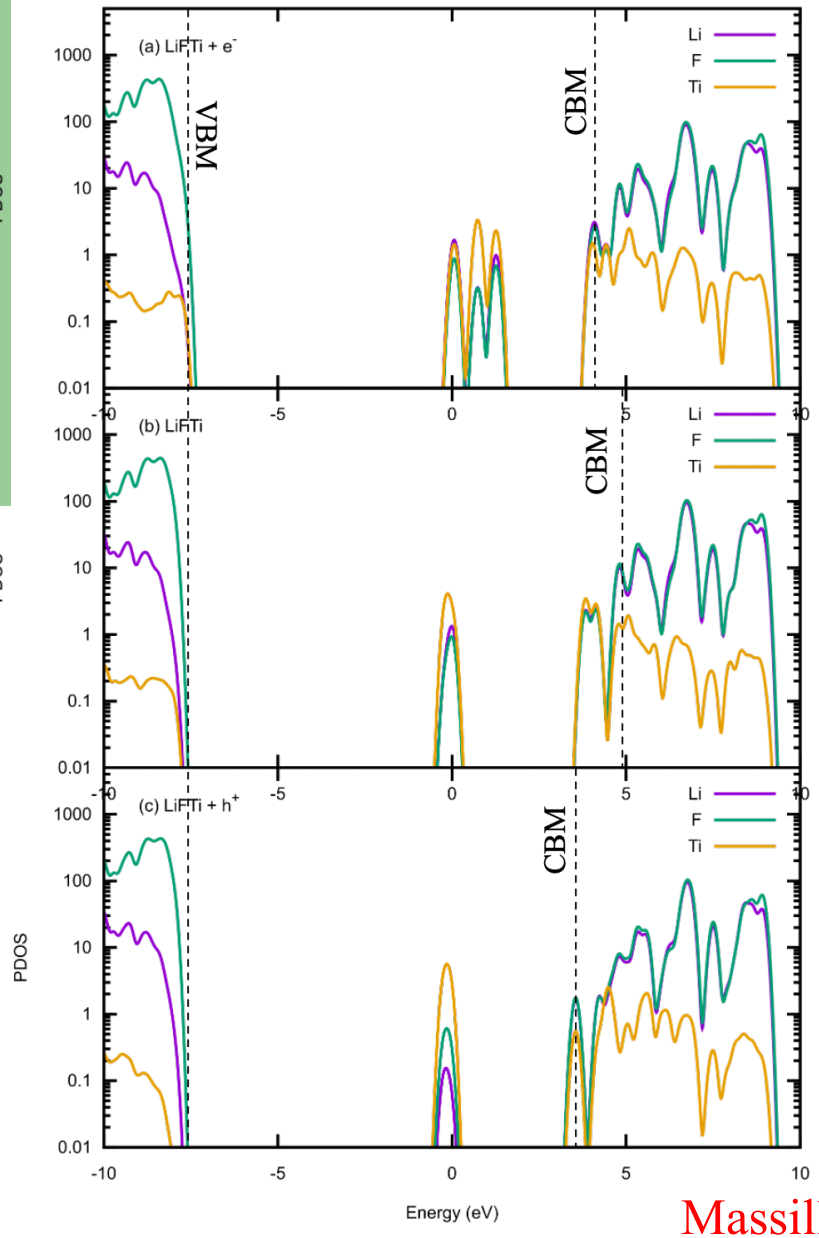

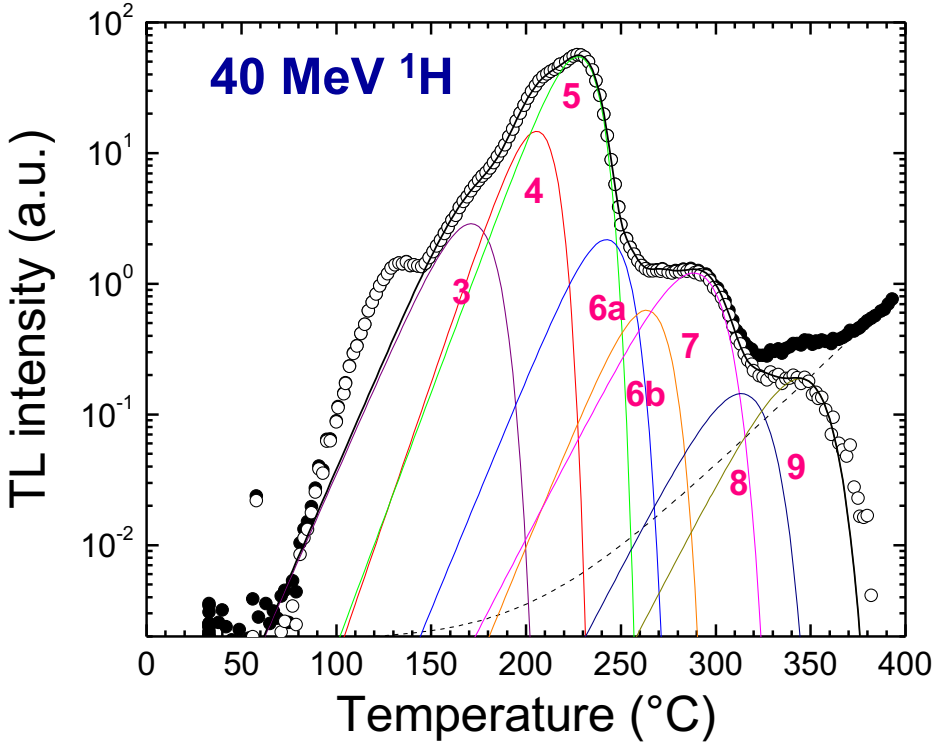

G Massillon-JL, PhD Thesis UNAM 2006

Massillon-JL et *al. Radiat. Meas.* **174** (2024) 107114

Defect states and electron localization in LiF:Ti

Spin density isosurface: Ti *4p*-state

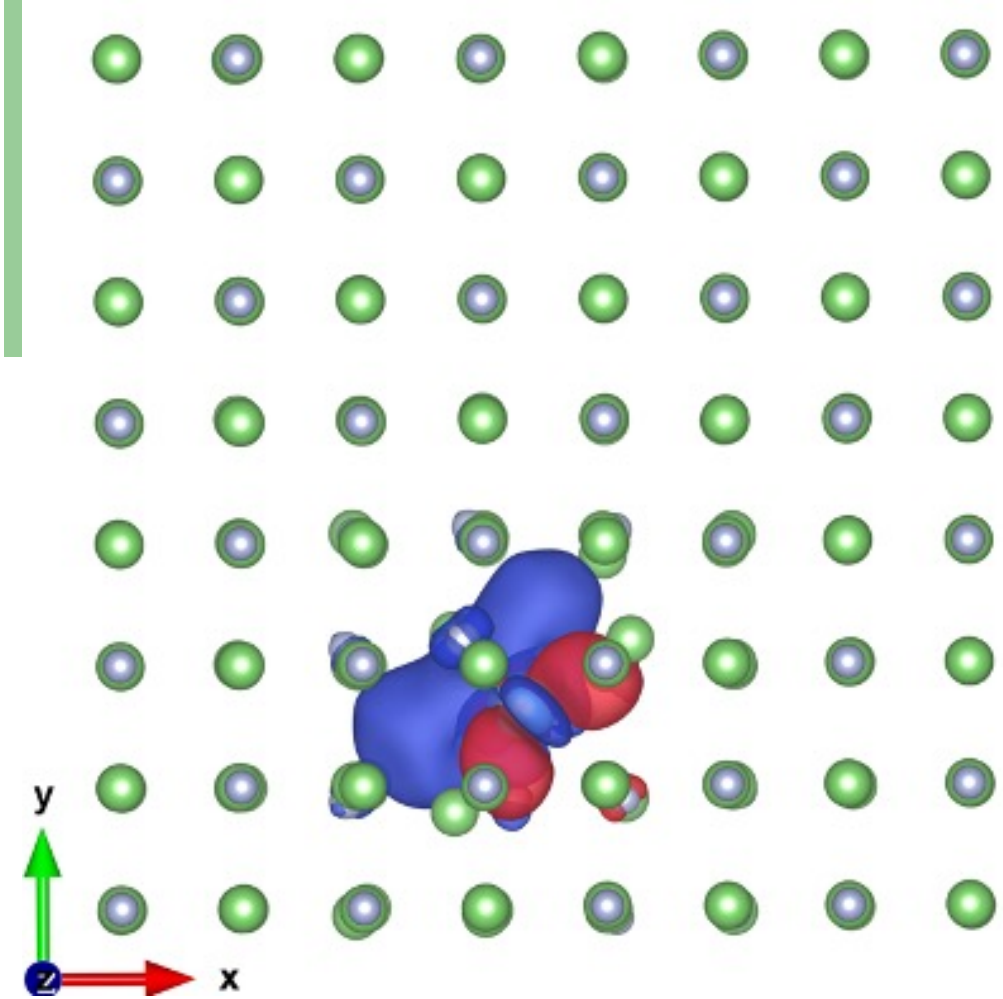

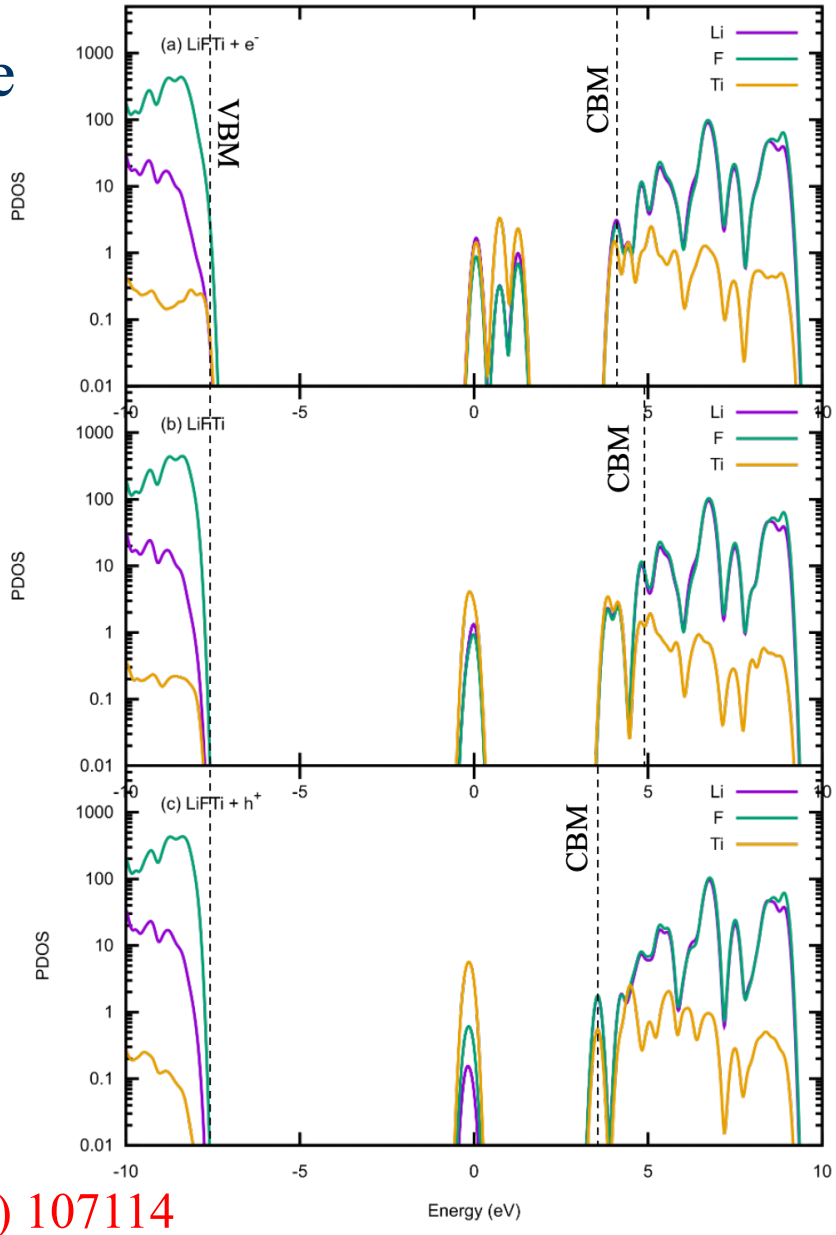

Massillon-JL et *al. Radiat. Meas.* **174** (2024) 107114

Defect states and hole localization in LiF:Ti

Spin density isosurface: Ti *3d*-state

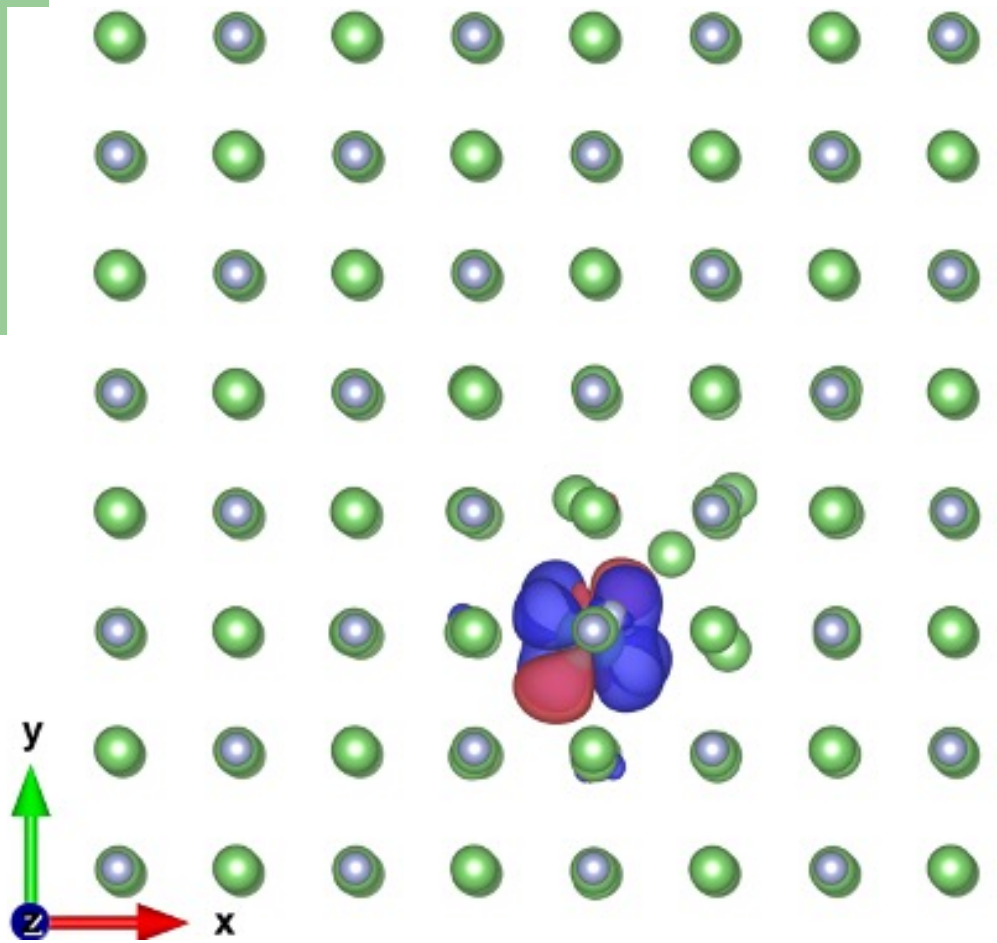

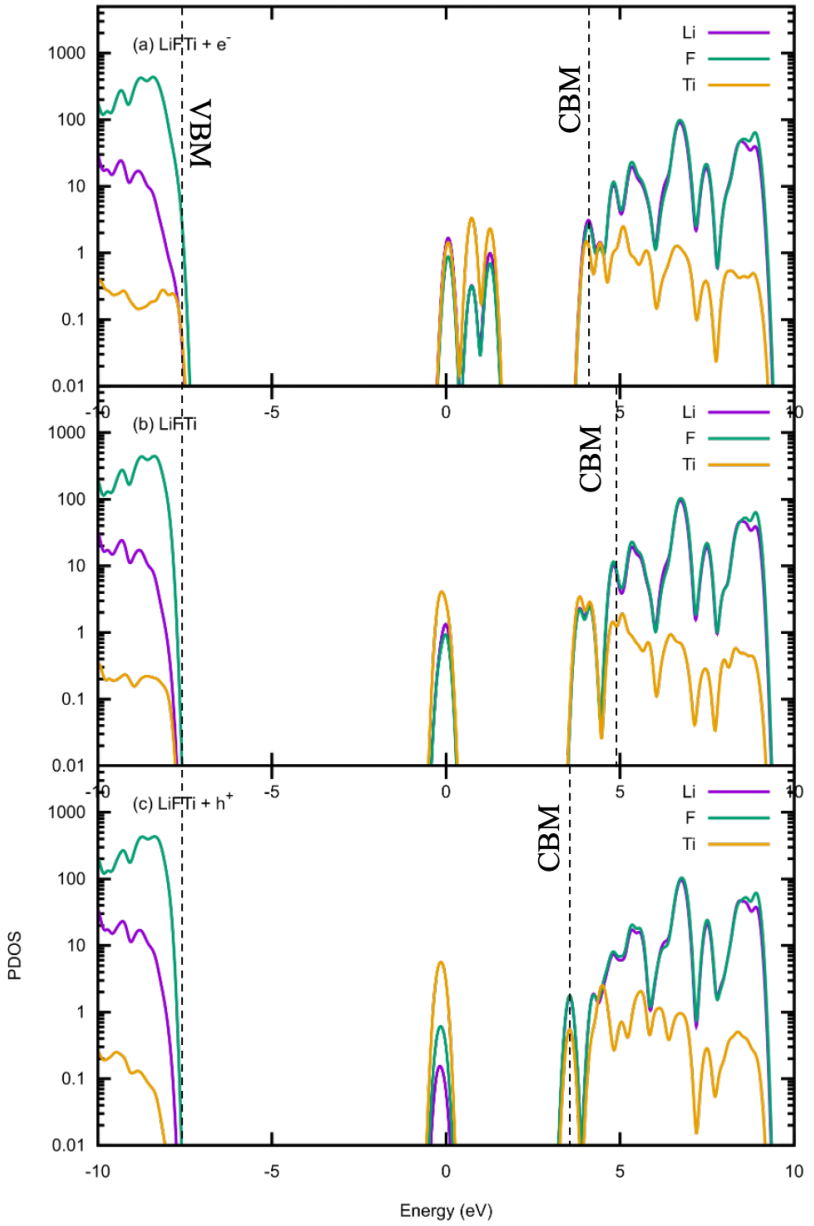

Massillon-JL et *al. Radiat. Meas.* **174** (2024) 107114

Defect formation energies

Defect formation energy and Thermodynamic transition level, $\varepsilon^{therm}(q_1/q_2)$

$$E_f(X^q) = E_{tot}(X^q) - E_{tot}(bulk) - \sum_i n_i\mu_i + qE_F$$

$$E_f\left(X^0; E_F = \varepsilon^{therm}(0/-1)\right) = E_f\left(X^{-1}; E_F = \varepsilon^{therm}(0/-1)\right)$$

$$\varepsilon^{therm}(0/-1) = E_{tot}(X^{-1}) - E_{tot}(X^0) = [\varepsilon_{i+1}(N) + \varepsilon_{i+1}(N+1)]/2$$

E_{tot} (X^q) and E_{tot} (*bulk*) are the total energies of the system containing the defect, X, and of the perfect crystal, respectively

$\pm n_i$: number of atoms that have been added (+) or removed (-)

μ_i: chemical potentials

E_F : Fermi energy

E_f: Formation energy

$\varepsilon_{i+1}(N+1)$ eigenvalue of the highest occupied state of the (N+1)-electron system

Defect formation energy

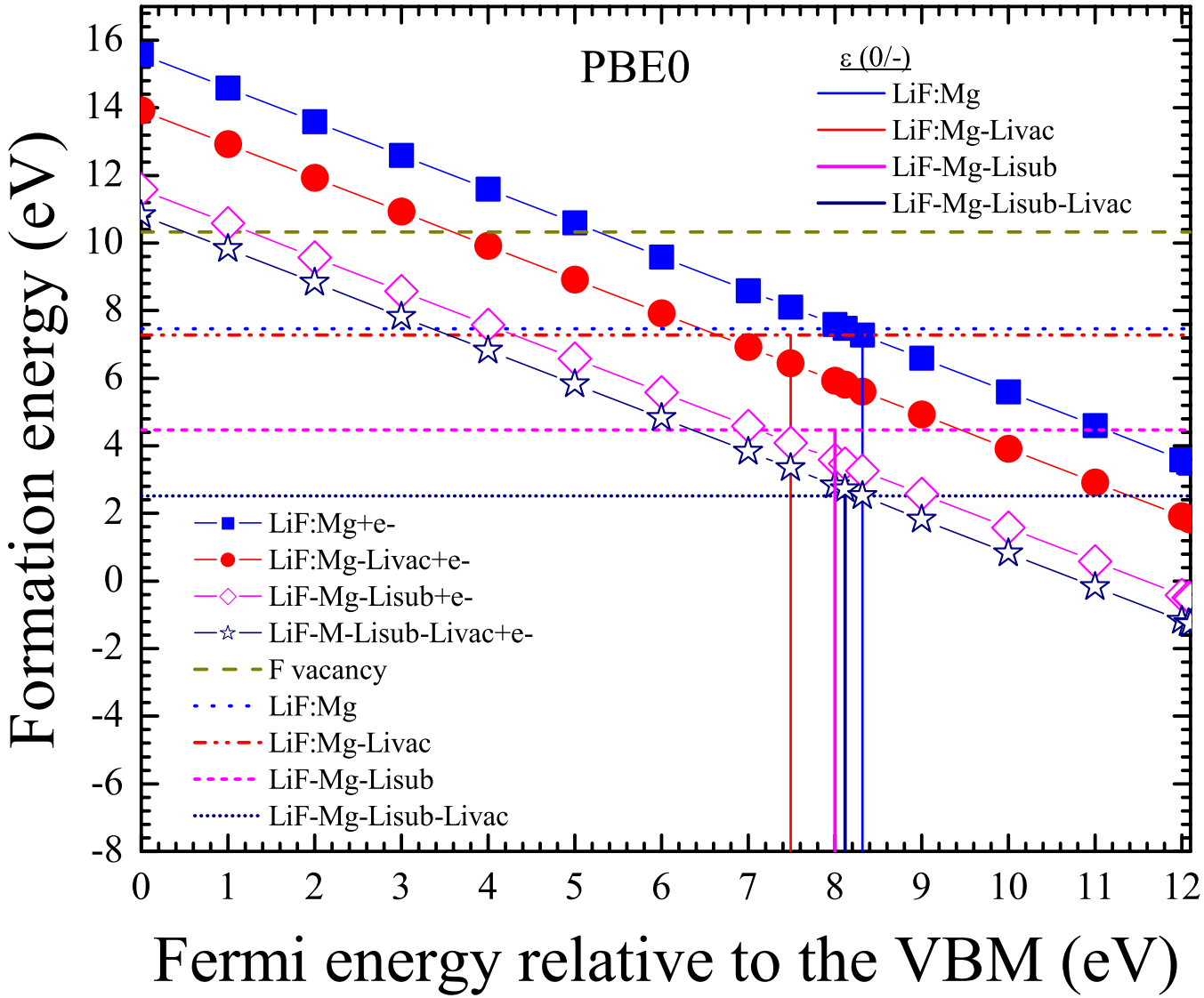

Massillon-JL et *al. J. Phys.:Condens. Matter* **31** (2019) 025502

Defect formation energy

Table 2. Defect formation energies, E_f, and thermodynamic transition levels, ε^{therm} (0/−1), of various defect-states in LiF at the PBE0 theory level. Energies in eV.

Defect-state	E_f ($E_F = 0$)	ε^{therm} (0/ −1)
LiF		
LiF-F vacancy	10.33	
LiF:Mg	7.463	
LiF:Mg + e^-	15.34	8.32
LiF:Mg–Li_{vac}	7.29	
LiF:Mg–Li_{vac} + e^-	13.92	7.49
LiF–Mg–Li_{sub}	4.48	
LiF–Mg–Li_{sub} + e^-	11.58	8.00
LiF–Mg–Li_{sub}–Li_{vac}	2.53	
LiF–Mg–Li_{sub}–Li_{vac} + e^-	10.83	8.11

Massillon-JL et *al. J. Phys.:Condens. Matter* **31** (2019) 025502

LiF:Mg, Summary

- The Mg interstitial creates a void for electron traps and is stable under normal conditions
- All charged defects are created by radiation and stables
- It is possible to identify the electron localization and quantify the energy loss for the defect's formation

Not all the energy deposited into the dosimeter's sensitive volume is transformed to a certain response

LiF:Ti, Summary

- In the presence of excess electrons, Ti stays in an interstitial position.
- Excess electrons are localized in the Ti 4*p*-orbitals
- In the presence of holes, Ti becomes a substitutional Li atom and the Li is moved to a tetrahedral interstitial position.
- Holes are localized in the Ti 3*d*-orbitals which are recombination centers

Ti dopant plays a dual character in LiF when exposed to ionizing radiation

Posgrado en Ciencias Físicas UNAM

Formatos para descarga

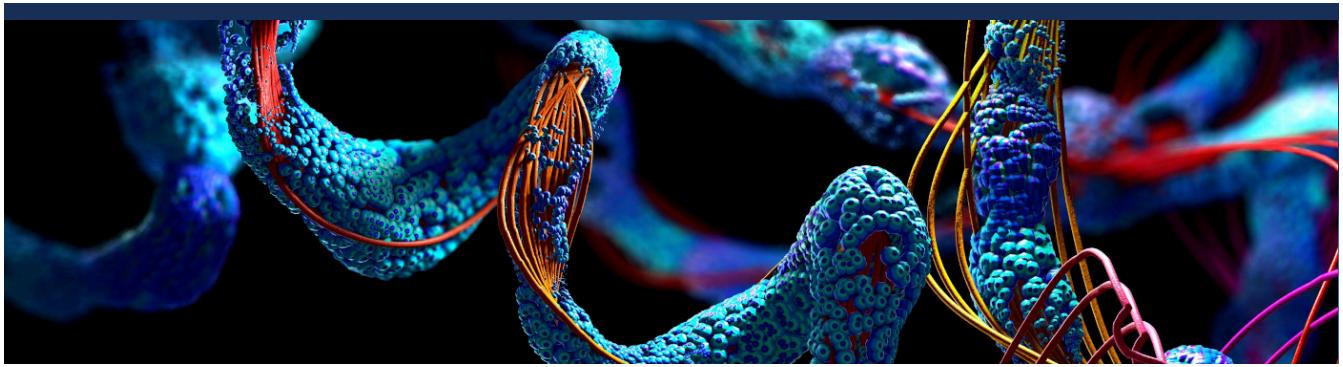

Maestría en Ciencias Físicas

El egresado de esta maestría tendrá: Conocimiento sólido conceptual y operativo de la Física, en general, así como del campo de conocimiento seleccionado, en particular. Alta capacidad en el manejo de metodologías y técnicas teóricas o experimentales, particularmente **ver más...**

Más Información

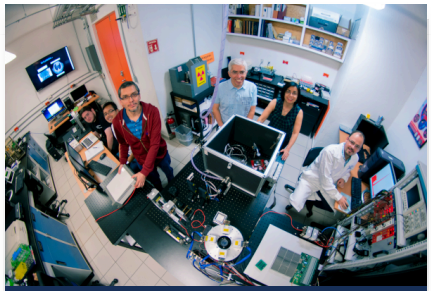

Maestría en Física Médica

El egresado de esta maestría tendrá una formación básica y un dominio conceptual, y operativo de las aplicaciones de la Física en Medicina, que permitirá su futuro desempeño como Físico Médico Clínico en servicios de tratamiento y diagnóstico de enfermedades, o como profesional **ver más...**

Más Información

Doctorado en Ciencias Físicas

El egresado de este doctorado habrá adquirido un sólido dominio conceptual y operativo de la Física, así como un conocimiento profundo y actualizado de su línea de investigación. Asimismo, prepara al alumno para realizar labores de docencia y de divulgación de alto nivel académico. **ver más...**

Más Información

Contacto:

Coordinación del Programa de Posgrado en Ciencias Físicas.
Correo: pcf@posgrado.unam.mx
Teléfono: 55-5623-7016, extensión 80045 y 55-5622-5134
Dirección:
Oficina Unidad de Posgrado
Edificio D, 1er piso, Circuito de los Posgrados, Ciudad Universitaria, Alcaldía Coyoacán, C.P. 04510, Cd. Mx., México.

Oficina Instituto de Física
Edificio Marcos Moshinsky, Circuito Exterior, Ciudad Universitaria, Alcaldía Coyoacán, C.P. 04510, Cd. Mx., México.

https://www.posgrado.fisica.unam.mx

Convocatoria

POSDOC 2024
POSDOC 2023
POSDOC 2022
POSDOC 2021

PREGUNTAS FRECUENTES

Inicio / Formación académica / POSDOC

Programa de Becas Posdoctorales en la UNAM (POSDOC)

Objetivo:

Fortalecer el quehacer científico y docente de alto nivel, apoyando a recién doctorados y doctoradas para que desarrollen un proyecto de investigación novedoso en la UNAM.

Dirigido a:

Recién doctorados y doctoradas de cualquier institución de reconocido prestigio, dentro de los cinco años previos a la fecha de inicio de la estancia posdoctoral; deberán tener una productividad demostrada por medio de obra publicada o aceptada para su publicación en revistas especializadas de prestigio internacional u otros medios de reconocida calidad académica y no deberán de tener contrato de trabajo con la UNAM al momento de iniciar la beca ni durante el periodo de la estancia.

Duración:

Un año, con posibilidad de una renovación por un año más, improrrogable.

Ingreso al GeDGAPA
Servicios en línea

Fechas destacadas POSDOC

ENE 27 Lun — POSDOC - Resultados - Renovaciones Periodo 2024 - II

https://dgapa.unam.mx/index.php/formacion-academica/posdoc